

Article

Assessment of the Impact of Lubricating Oil Contamination by Biodiesel on Trunk Piston Engine Reliability

Leszek Chybowski ^{1,*} , Przemysław Kowalak ^{2,*} and Piotr Dąbrowski ³¹ Department of Machine Construction and Materials, Faculty of Marine Engineering, Maritime University of Szczecin, ul. Willowa 2, 71-650 Szczecin, Poland² Department of Marine Power Plants, Faculty of Marine Engineering, Maritime University of Szczecin, ul. Willowa, 71-650 Szczecin, Poland³ Independent Researcher, 71-650 Szczecin, Poland; piotr.j.dabrowski@icloud.com

* Correspondence: l.chybowski@pm.szczecin.pl (L.C.); p.kowalak@pm.szczecin.pl (P.K.)

Abstract: The rheological, ignition, and tribological properties of lubricating oils diluted with biodiesel were analyzed. The flash point t_{FP} , calculated cetane index CCI , density ρ , coefficient of the temperature density change ε , kinematic viscosity ν , dynamic viscosity η , viscosity index VI , and lubricity during a High-Frequency Reciprocating Rig (HFFR) test (x , y , WSD , and $WS_{1.4}$) and lubricating conditions during an HFFR test (oil film resistance $FILM$ and friction coefficient μ) were determined. The test was performed for the oil mixtures of the lubricating oil of the SAE 30 and SAE 40 viscosity grades, which were diluted with the biodiesel blend (D93B7—diesel oil with 7% v/v fatty acid methyl esters, FAME) at concentrations of diesel oil in the mixture equal to 0% (pure lubricating oil), 1%, 2%, 5%, 10%, 20%, 30%, 50%, and 75% m/m , respectively. The experiment confirmed the existence of clear relationships between the increase in the dilution of lubricating oil with tested biodiesel blend and t_{FP} , ρ , ε , ν , η , and VI , and the deterioration of lubrication conditions. It is recommended to take remedial action even in the case of low diesel oil concentration (<5% m/m) in the lubricating oil due to t_{FP} , ν , and η changes. Simultaneously, the tests showed no significant effect on the lubricity and the CCI . The critical contamination of oil with fuel in the range of 2–5% by weight, as indicated in the literature, still allowed for a certain “safety margin” regarding these parameters. However, when the concentration of diesel fuel in the lubricating oil exceeded 5–8% m/m , the deterioration of the lubrication was expressed by a decrease in $FILM$ and an increase in μ was observed; hence, such a contamination should be considered excessive. When the concentration of diesel fuel exceeds 10% by weight, there is a serious risk of engine damage during operation.

Keywords: crankcase explosion; lubricating oil properties; oil dilution with distillation fuel; high-frequency reciprocating rig; HFFR; mechanical wear; anti-wear properties; lubricity



Citation: Chybowski, L.; Kowalak, P.; Dąbrowski, P. Assessment of the Impact of Lubricating Oil Contamination by Biodiesel on Trunk Piston Engine Reliability. *Energies* **2023**, *16*, 5056. <https://doi.org/10.3390/en16135056>

Academic Editor: Nadir Yilmaz

Received: 26 May 2023

Revised: 20 June 2023

Accepted: 28 June 2023

Published: 29 June 2023



Copyright: © 2023 by the authors. Licensee MDPI, Basel, Switzerland. This article is an open access article distributed under the terms and conditions of the Creative Commons Attribution (CC BY) license (<https://creativecommons.org/licenses/by/4.0/>).

1. Introduction

The issue of the impact of lubricating oil dilution with diesel oil with respect to an increase in the explosion risk in the engine crankcase has not been clearly presented so far in the literature. Crankcase explosions in trunk pistons and crosshead engines still occur; thus, the subject remains topical [1]. The possibility of contamination of the lubricating oil with the fuel supplying the engine primarily applies to trunk piston engines [2], where the combustion chambers are directly separated from the crankcase by piston rings [3]. Damage to the rings results in exhaust gas, air, and fuel blowing into the crankcase.

There are two extreme approaches in the literature to the subject of lubricating oil contamination by diesel oil, and the effects of this contamination on engine operation [4], e.g., the seizing of bearings in the crank-piston system [5]. The first is the approach presented in a paper published by Ferguson [6] and by CIMAC [7]. This procedure states that the effects of diesel contamination in lubricating oil are negligible, even at high diesel

concentrations in the lubricating oil. The second approach points to an increased risk of engine seizure [8–10]. In some sources, 2–5% diesel content in the lubricating oil is an alarming level and requires immediate maintenance [11,12]. Castrol [13] and some other companies [14] report that dilution of lubricating oil with fuel exceeding 8% can result in an explosion in the crankcase. However, neither approach is sufficiently well argued; a holistic approach to the subject has not been presented.

Whereas the truth usually lies “somewhere in the middle”, the extreme approaches of the above research groups do not reflect the actual situation. In an attempt to answer the question regarding the existence of the influence of distillation fuel on the properties of contaminated lubricating oil and the related impact of the lubricating oil contamination with diesel on engine operation, research work has been undertaken. The outcomes of the research, among others, are presented elsewhere (failure prevention methods [8], oil volatility influence [15], oil rheological properties influence [16]).

Moreover, changes in the lubrication conditions of the elements of the tribological systems pistons, piston rings, and cylinder liner may result in an increase in the temperature of these elements and the formation of hot spots in the lower part of the cylinder liners, which in turn contributes to the intensification of the oil evaporation and the formation of oil mist in the crankcase. This aspect, in addition to mechanically generated mist, is one of the factors leading to the formation of an explosive oil–air mixture in the crankcase; it is a source of energy to initiate the ignition of this mixture.

Seizure of the tribologically coupled elements (here, the pistons, piston rings, and cylinder liners) is associated with an excessive increase in the working surface temperature (due to lubricating oil viscosity drop [5] or lubricating oil contamination [17]). Thermal energy transferred via conduction is described, with a good approximation, by the Fourier differential equation [18], i.e.,:

$$\frac{\partial Q}{\partial \tau} \approx -\lambda \oint_A \nabla T \cdot dA, \quad (1)$$

where Q represents thermal energy (in units J), τ signifies time (s), λ is the thermal conductivity coefficient ($W/(m \cdot K)$), A is the heat transfer surface (m^2), T is the absolute temperature (K), ∇ is the vector differential operator (nabla), and $\nabla T = \text{grad } T$ is the temperature field gradient.

For steady heat flow through a flat wall, after integrating and changing the temperature scale to relative temperature expressed in $^{\circ}C$, Equation (1) has the following form:

$$\dot{Q} = \frac{\lambda A}{d} \Delta t, \quad (2)$$

where \dot{Q} denotes the heat stream (W), d is the wall thickness of the heat conductor (m), and Δt is the temperature difference on both sides of the heat conductor ($^{\circ}C$). For a steady flow through the cylindrical wall of the liner (cylinder liner), Equation (1) becomes:

$$\dot{Q} = \frac{2\pi l \lambda}{\ln\left(\frac{d_2}{d_1}\right)} \Delta t = \dot{q} A, \quad (3)$$

where l signifies the length (height) of the liner (m), d_1 is the diameter of the cylinder liner on the warmer side (m), d_2 is the diameter of the cylinder liner on the cooler side (m), and \dot{Q} is the unit heat stream (W/m^2).

The unit heat stream of friction \dot{q} ($J/(s \cdot m^2)$) is described by the following formula [19]:

$$\dot{q} = C_m p \mu = S_{gr} \mu, \quad (4)$$

where C_m denotes the average planning speed (m/s), p is the unit pressure (Pa), S_{gr} is the factor of proportionality, and μ is the friction coefficient (–).

The mathematical derivation of Equation (4) is presented in Appendix A.
The friction coefficient is defined as:

$$\mu = \frac{F}{P}, \quad (5)$$

where F is the friction force (N) and P is the pressure force (N). For a given tribological pair, the heat stream delivered to surface A that rubs against surface B (made of any material), according to the relations (2) and (3), will induce along this element the temperature distribution t_A (°C)– t_B (°C). The latter is defined by the following relationship [19]:

$$t_A - t_B = \frac{\dot{q}}{\lambda}. \quad (6)$$

In order for a seizure to occur on surface A, the surface must reach a melting temperature of t_{top} (°C) for which:

$$t_{top} - t_0 = \frac{\dot{q}}{\lambda}, \quad (7)$$

where t_0 is a constant temperature of the surface B, which is equal to the surface of the piston on the side of the gases, at approximately 350–450 °C. Taking the average value and substituting Equations (4) into (7), the obtained formula for factor S_{gr} [19] is:

$$S_{gr} = pC_m = \frac{\lambda}{\mu} (t_{top} - 400). \quad (8)$$

During a seizure, the material is plasticized, which forms welds between the irregularities on the material surfaces and ultimately results in the bonding of the components or their tearing and the transfer of material from one component to another (thermal properties of the materials [20], materials combustibility [21]). The limiting values of the S_{gr} coefficient, calculated from Equation (8), are summarized in Table 1.

Table 1. S_{gr} values for selected material vapors (prepared based on [22]).

Pair of Materials	Coefficient of Dynamic Dry Friction (–)	Melting Point t_{top} (°C)	Thermal Conductivity Coefficient λ (W/(m · K))	Coefficient S_{gr} (W/m ²)
Cast iron	~0.18	1200	55	0.245
Cast iron		1200	55	0.245
Cast iron	0.18	1200	55	0.245
Steel		1400	40	0.221
Cast iron	0.08	1200	55	0.550
Chrome		1920	92	1.755
Cast iron	~0.10	1200	55	0.442
Molybdenum		2620	142	3.140

If the fuel in the oil worsens the wear conditions of the piston–piston rings–cylinder liner system due to thinning of the oil film, then fuel contamination may be the cause of engine seizure. Previous work [16] has indicated that when the diesel oil content in the lubricating oil exceeds 10%, an oil film rupture occurs, which can result in increased wear for the tribological couples, such as the bearings in the crank–slider system. At the same time, given the decrease in viscosity and, thus, the deterioration of the lubrication conditions and the reduction in the evaporation and ignition temperatures, one can conclude that the synergistic interaction of these factors increases the risk of explosion in the engine crankcase. Previous work [23] has presented a middle ground for the earlier-mentioned extreme opinions regarding the impact of diesel oil contamination on engine performance and, simultaneously, the obtained results show that diesel oil levels are above 10% when oil film rupture occurs and can be classified as critical.

The results also showed a clear relationship between the flash point and the rheological indexes of the oil contaminated with distillate fuel at different contamination levels. In the latter group of indicators, for the SAE 30 and SAE 40 oils most commonly used in the lubrication systems of marine engines, the changes in density, kinematic viscosity, dynamic viscosity, viscosity index, and the coefficient of temperature change in density are analyzed and interpreted in the context of increased contamination of the lubricating oil with diesel oil.

Simultaneously, in [23], an analysis of the selected quantities describing the tribological properties of the mixture is carried out, namely, the results of the mixture's lubricity tests that are performed with the use of a High-Frequency Reciprocating Rig (HFFR). At the same time, additional parameters obtained during this test are analyzed. This includes the percentage resistance of the oil film separating the samples (i.e., the *FILM* parameter showing the change in the oil film thickness) during the lubricity test and the average coefficient of friction of the samples that are separated by the tested liquid during the lubricity test.

The determined results did not show a clear relationship with the lubricity. However, they indicated changes in the value of additional parameters. Nevertheless, these values for the coefficient of friction showed a significant increase at diesel oil concentrations above 10% m/m, and then decreased at high diesel oil concentrations (pure diesel oil). On the other hand, the *FILM* parameter for the tested SAE 30 oil with contamination above 10% m/m of diesel oil in lubricating oil decreased in the entire concentration range, while it initially decreased and then increased its value for SAE 40 oil. Nevertheless, for both the tested oils, when the diesel oil concentration was exceeded by 10% m/m, the value of the *FILM* parameter did not reach the values obtained for the diesel oil concentrations not higher than 10%.

The explanation for this effect may lie in the synergistic effect of the oil and diesel oil components on the properties of the mixture of these two products. This may be related to the interaction and the interplay of enriching additives in lubricating oils and additives modifying diesel oil properties, which change, among others, the contact angle between the liquid and the working element. In operating conditions, the contamination of the lubricating oil with diesel oil (exceeding 10% m/m) is usually unheard of when the engine is used and serviced properly. However, wanting to investigate the relationship between the level of contamination of the lubricating oil with the diesel oil and the tribological and rheological properties of such a mixture, additional tests were carried out with more samples and a high diesel oil content in the lubricating oil. Simultaneously, pure diesel oil is removed from the comparative analyses, as it differs significantly in its characteristics when compared to the properties of the lubricating oil–diesel oil mixtures.

To clarify the nature of the changes in the lubricity of the lubricating oil with the dilution of the lubricating oil with diesel oil, as indicated in [16], this article presents a greater number of measurements, providing and analyzing lubricity test results for mixtures over a wide range of diesel oil concentrations, namely, 0%, 1%, 2%, 5%, 10%, 20%, 30%, 40%, 50%, 75%, and 100% m/m of diesel oil. In addition to the *WSD* lubricity, the corrected *WS_{1.4}* lubricity and the baseline wear values in two orthogonal wear directions (i.e., *x* and *y*) were provided to obtain a complete picture of lubricity. Additionally, in the full range of concentrations, the relative percentage film thickness (*FILM*) and the average friction coefficient μ during HFFR tests were determined.

These studies also resulted in obtaining additional results regarding the ignition properties. Previously, the calculated cetane index (*CCI*) values were determined only for 50% contamination of the lubricating oil and for pure diesel oil. The additional research provided insight into the changes in the *CCI* parameter for the dilution of the lubricating oil with diesel oil above 30–40% m/m of diesel oil content in the mixture.

Furthermore, this article provides a comprehensive assessment of all oil indicators. In addition to the aforementioned characteristics of ignition and tribological properties, the results of rheological indicators were also presented, including kinematic viscosity

ν , dynamic viscosity η , density ρ , the temperature coefficient of density change ε , and viscosity index VI. All results were summarized, their variability was described, and the correlation of their changes with the level of lubricating oil contamination with diesel oil was presented.

The results of the experiment are included in Appendix B, with the comparative data in the associated dataset obtained from earlier studies [24]. Slight differences in the data indicate that these sources (for the same measurement points) result from a slightly different composition of the diesel oil used in the current experiment. Detailed information on the lubricating oil and diesel oil used to produce the analyzed mixtures is presented in the Materials and Methods section.

2. Materials and Methods

2.1. Analyzed Mixtures of the Lubricating Oil and Diesel Oil

In the experiments, the properties of the SAE 30 and SAE 40 lubricating oils were tested using clean (0% diesel oil) and contaminated lubricating oil in the amounts of 1%, 2%, 5%, 10%, 20%, 30%, 50%, and 75% m/m diesel oil in the mixture. The Orlen Efecta Diesel Bio (7% FAME) oil was used [25], which meets the requirements of the regulation “RMG for liquid fuels” [26] and the ZN-ORLEN-5:2019 standard [27], and Emi/Agip Cladium 120 SAE 30 API CF and Emi/Agip Cladium 120 SAE 30 API CF lubricating oils meet the viscosity requirements of the SAE J-300 classification [28]. The properties of the oils used are listed in Tables 2 and 3.

Table 2. Properties of the diesel oil used in the tests.

Specification of Orlen Efecta Diesel Bio	Declared Value by the Manufacturers [8]	Measured Value [16]
Cetane index	≤ 51	52
Initial boiling point	75–180 °C	181 °C
Boiling temperature range	92% vol. distills is 360 °C 36% vol. distills is 250 °C	
Flash point (determined in a closed cup)	62 °C	65 °C
Auto-ignition temperature (according to DIN51794:2003-05 [29])	approx. 240 °C	
Kinematic viscosity (according to PN-EN ISO 3104:2021-03 [30])	1.5–4.5 mm ² /s (2.549 mm ² /s) at 40 °C approx. 2151 mm ² /s at 50 °C	2897 mm ² /s at 40 °C 2443 mm ² /s at 50 °C
Density	820–845 kg/m ³ at 15 °C	835.81 kg/m ³ at 15 °C
Relative vapor density	approx. 6 (air = 1)	
Cloud point	−8 °C	
Cold filter plugging point	−28 °C	
Residual ash (from 10% distillation rests)	0.010% m/m	
FAME additives	max. 7% v/v	
Lubricity WD _{1.4}	415 µm at 60 °C	213 µm at 60 °C

Table 3. Properties of the lubricating oil used in tests.

Oil	Specification	Declared Value by the Manufacturer [31–33]	Measured Value [16]
Emi/Agip Cladium 120 SAE 30 API CF	Kinematic viscosity (according to EN ISO 3104)	108 mm ² /s at 40 °C 12.0 mm ² /s at 100 °C	105.01 mm ² /s at 40 °C 11.72 mm ² /s at 100 °C
	Viscosity index	100	99.3
	Base number	12 mg KOH/g	
	Flash point	225 °C	
	marked in the open cup		
	marked in the closed cup		180 °C
	Pour point	−18 °C	
	Density	895 kg/m ³ at 15 °C	898.29 kg/m ³ at 15 °C

Table 3. Cont.

Oil	Specification	Declared Value by the Manufacturer [31–33]	Measured Value [16]
Emi/Agip Cladium 120 SAE 40 API CF	Kinematic viscosity (according to EN ISO 3104)	160 mm ² /s at 40 °C 15.7 mm ² /s at 100 °C	159.90 mm ² /s at 40 °C 15.21 mm ² /s at 100 °C
	Viscosity index	100	95.3
	Base number	12 mg KOH/g	
	Flash point	235 °C	
	marked in the open cup		
	marked in the closed cup		178 °C
	Pour point	−15 °C	
	Density	900 kg/m ³ at 15 °C	898.44 kg/m ³ at 15 °C

The rheological, tribological, and ignition properties were determined for each oil sample. The flowchart outlining the procedure adopted for conducting the tests is presented in Figure 1.

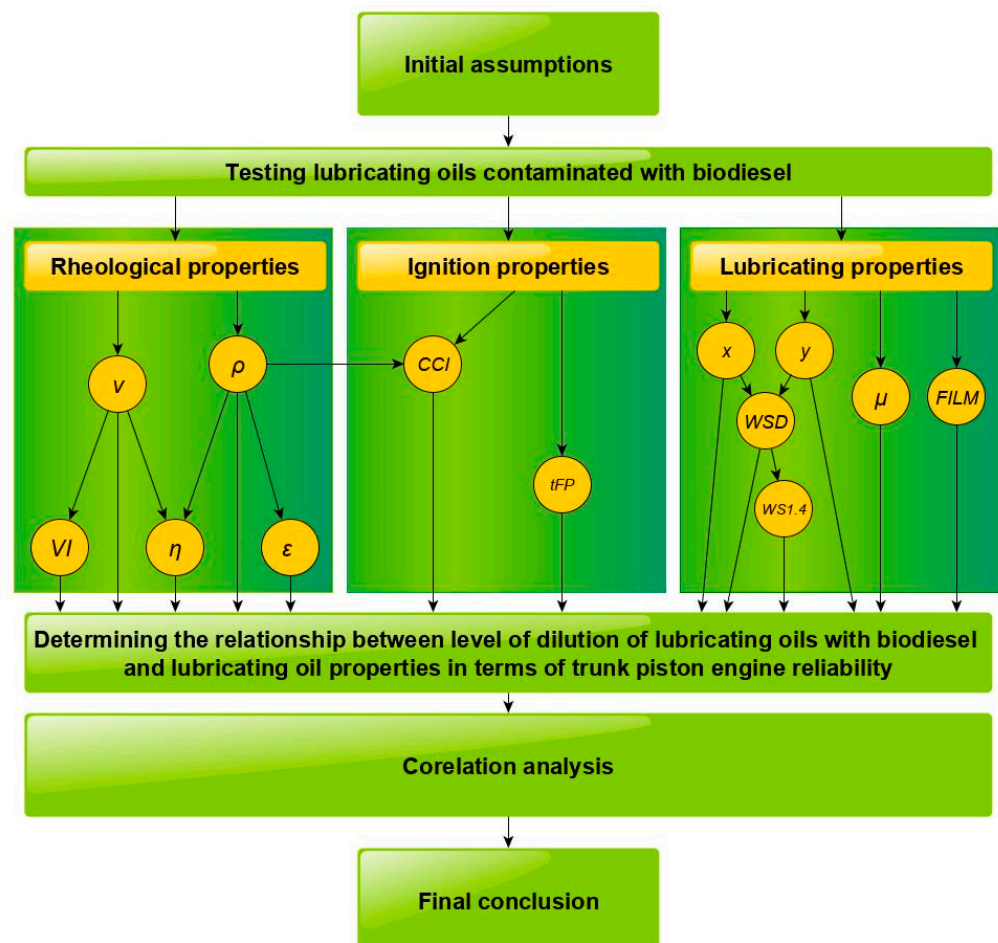


Figure 1. Research methodology adopted (description in text).

Laboratory tests were performed on behalf of the authors at the Center for Testing Fuels, Working Fluids, and Environmental Protection (CBPCRiOŚ) of the Maritime University of Szczecin. Standardized measurement methods were applied. A list of standards and procedures in accordance with which the tests were conducted are presented in Table 4.

Table 4. Standards applied in laboratory tests.

Measured Parameter	Standard or Procedure Applied
Flash point temperature (t_{FP})	PN-EN ISO 2719:2016 [34]
Calculated cetane index (CCI)	ASTM D4737-21 [35]
Density (ρ)	PN-EN ISO 12185:2002 [36]
Temperature density change (ϵ)	PN-EN ISO 12185:2002 [36] and calculations
Kinematic viscosity (ν)	PN-EN ISO 3104:2004 [30]
Dynamic viscosity (η)	PN-EN ISO 12185:2002 [36], PN-EN ISO 3104:2004 [30], and calculations
Viscosity index (VI)	ASTM D2270-10(2016) [37] and Anton Paar calculator
Lubricity ($x, y, WSD, WS_{1.4}$)	ISO 12156-1:2018 [38]
Oil film resistance drop (FILM)	Procedure implemented in PCS HFFR V1.0.3 apparatus
Friction coefficient (μ)	Procedure implemented in PCS HFFR V1.0.3 apparatus

For individual measured values that characterize the ignition, rheological, and tribological properties, their correlation with the diesel oil content in the tested mixture of the lubricating oil and the diesel oil (% m/m of the diesel oil) is determined. Pearson's correlation coefficient, r_{XY} , is used for this purpose and is given by:

$$r_{XY} = \frac{\text{cov}(X, Y)}{\sigma_X \cdot \sigma_Y}, \quad (9)$$

where $\text{cov}(X, Y)$ represents the covariance of variables X and Y , and σ_X and σ_Y are the standard deviations of variables X and Y , respectively. The strength of the correlations adopted in this article is interpreted in accordance with the assumptions presented in Table 5.

Table 5. Assumed Pearson correlation coefficient interpretation.

The Value of Pearson's Coefficient r_{XY}	Interpretation of the Relationship between Two Variables
$0.000 \leq r_{XY} < 0.200$	Very low correlation. No relationship.
$0.200 \leq r_{XY} < 0.400$	Low correlation. The relationship is clear.
$0.400 \leq r_{XY} < 0.600$	Moderate correlation. Significant dependence.
$0.600 \leq r_{XY} < 0.800$	High correlation. Significant dependence.
$0.800 \leq r_{XY} \leq 1.000$	Very high correlation. Very high-to-full dependency.

2.2. Ignition Properties of the Oil Diluted with Diesel Oil

According to EN IEC 60079-10-1 [39], the flash point of a material is the lowest liquid temperature at which, under certain standardized conditions, a liquid emits vapors in a quantity that is capable of forming an ignitable vapor/air mixture. If the substance tested is the lubricating oil contaminated with the diesel oil in the amount of C (% m/m), the flash point temperature t_{FP} can be provided as a function of the contamination of the lubricating oil with diesel fuel, and the auto-ignition temperature decreases with the increasing value of C [15].

As indicated in the literature recommendations, the flash point of lubricating oil should not drop below ca. 180 °C measured in a closed cup [40] or ca. 220 °C. measured in an open cup [41]. The results of the flash point measurement in the closed cup are usually ca. 20–40 °C lower than the results in the open cup [42].

In this experiment, the flash point was determined in accordance with PN-EN ISO 2719:2016 [34] in a closed cup using the Pensky–Martens method. To perform the test, the Flashpoint Pensky–Martens Semi-Automatic apparatus was used (Walter Herzog GmbH, Lauda-Königshofen, Germany). According to the latest certification results of the apparatus, the measurement accuracy is 0.10% and the repeatability is 0.10 K (0.10 °C) for the range 363.15–643.15 K (90–370 °C), while this accuracy is 0.35% and the repeatability is 0.05 K (0.05 °C) for the range 268.15–383.15 K (−5–110 °C) [15].

The second parameter, determined as part of the experiment, which provides the ignition properties of the tested mixtures is the index describing the delay of the self-ignition in test conditions, at a temperature higher than the so-called auto-ignition temperature. Self-ignition is the spontaneous beginning of the combustion process of a substance without the participation of an external source ignition, such as a flame or a spark. The auto-ignition delay is defined as the time that occurs between the spray of the combustible substance and the start of the combustion process after the auto-ignition has occurred. The indicator that describes the self-ignition delay is the cetane number (or cetane rating), which is determined using special CFR test engines. For marine fuels, it is assumed that a CN value above 45 corresponds to very good ignition properties, while 40–45 is good to very good, 35–40 is acceptable to good, 28–35 is bad to acceptable, 25–28 is very bad to bad, and below 25 is very bad or unfit for use.

Due to the cost of the apparatus, many indicators that describe the self-ignition delay are used to accurately determine the cetane number, which is determined using the dedicated test analyzers (derived cetane number, *DCN*) and the laboratory methods (cetane index, *CI*, and calculated cetane index, *CCI*), and also the approximate calculation formulas for residual fuels (calculated ignition index, *CII*, and calculated carbon aromaticity index, *CCAI*) [43]. In this experiment, the determination of the value of the derived cetane number (*DCN*) [44,45] was not possible for mixtures of lubricating oils with diesel oil contamination due to the technical limitations of the device and the flammability properties of mixtures with a low content of diesel oil in the mixture.

The *CCI* index was chosen as the critical parameter, which is determined in accordance with the ASTM D4737-21 standard based on the volatility of the substance [46] and is described by the withdrawal temperatures of 10%, 50%, and 90% *v/v* of the test mixture during distillation [35]. The *CCI* indicator is interpreted analogously to the *CN* [43] and is determined in accordance with the mentioned standard based on the four-variable equation [35], i.e.,:

$$CCI = 45.2 + 0.0892 \cdot (t_{10} - 215) + \{0.131 + 0.901 \cdot [e^{-3.5 \cdot (\rho_{15} - 0.85)} - 1]\} \cdot (t_{50} - 260) + \{0.0523 - 0.420 \cdot [e^{-3.5 \cdot (\rho_{15} - 0.85)} - 1]\} \cdot (t_{90} - 310) + 0.00049 \cdot [(t_{10} - 215)^2 - (t_{90} - 310)^2] + 107 \cdot [e^{-3.5 \cdot (\rho_{15} - 0.85)} - 1] + 60 \cdot [e^{-3.5 \cdot (\rho_{15} - 0.85)} - 1]^2, \quad (10)$$

where ρ_{15} (g/cm³) is the density at 15 °C and t_{10} , t_{50} , and t_{90} (°C) are the 10%, 50%, and 90% recovery temperatures, respectively.

In previous experiments, the determination of the *CCI* for mixtures of lubricating oil and diesel oil was possible only for mixtures with a content of diesel in the lubricating oil equal to or greater than 50% m/m [16], which results from the complex composition of the lubricating oils that are not a pure mixture of hydrocarbons (they contain a number of enriching additives). In this experiment, due to the increase in the number of measurement points, an attempt was made to determine the *CCI* value for a larger number of measurement points. *CCI* values were determined for the contents of 30%, 40%, 50%, and 75% m/m diesel oil in blends with SAE 30 grade lubricating oil and 40%, 50%, and 75% m/m diesel oil in blends with SAE 40 grade lubricating oil. The tests were performed using the Flashpoint Pensky–Martens Semi-Automatic apparatus mentioned above (from Walter Herzog GmbH, Lauda-Königshofen, Germany).

2.3. Rheological Properties of the Lubricating Oil Diluted with Diesel Oil

Rheology deals with the deformation of materials and their flow under the action of forces. Viscosity is the basic parameter that describes the fluidity of fluids. It is a property of fluids and plastic solids that characterizes their internal friction resulting from the sliding of fluid layers relative to each other during a flow [47]. The dynamic viscosity (absolute) η (mPa·s) is a measure of fluid resistance to dynamic loads [48]. Dynamic viscosity η is

calculated as the product of kinematic viscosity ν (mm²/s) and fluid density ρ (kg/m³) at a given measurement temperature t , so that:

$$\eta = \frac{\nu \cdot \rho}{1000}. \quad (11)$$

Viscosity is the most important quantity that characterizes fluid friction since it is responsible for separating the cooperating surfaces in friction conditions [49]. To create appropriate conditions for the cooperation of the tribological nodes, it is therefore necessary to maintain the viscosity above a certain minimum value [50]. Bearing in mind that the oil in the engine is selected for the expected engine operating conditions and the assumed load range, the use of the correct oil in accordance with the engine manufacturer's recommendations should ensure effective engine operation [19].

As indicated in the literature recommendations, the kinematic viscosity of lubricating oil in reference temperature (40 °C or 100 °C) should not change more than −10% to +10% [51] for caution and −20% to +30% [40] for a problem indication (alarm level) in relation to the viscosity of fresh oil.

In contrast, the seizing of the sliding parts may occur in the case of an excessive decrease in viscosity, which may occur as a result of the dilution of the lubricating oil with diesel oil, contamination of the lubricating oil with water, or excessive overheating of the oil (i.e., the thickness and viscosity of the oil decrease with increasing temperature) [42]. However, it must be noted that contamination does not always affect visible changes in viscosity [52]. To determine the dynamic viscosity, the kinematic viscosity and the density of each sample were measured. The kinematic viscosity of the individual samples in this experiment was determined in accordance with PN-EN ISO 3104:2004 [30] using a Cannon-Fenske Opaque glass capillary viscometer (from Paradise Scientific Company Ltd., Dhaka, Bangladesh) and a TV 2000 viscometric bath (from Labovisco bv, Zoetermeer, the Netherlands). The measured kinematic viscosity values were used to calculate the viscosity index [53] and the coefficient of temperature change in density [54].

The accuracy of the temperature setting is ± 0.01 °C, while the accuracy of the viscosity measurement is ± 0.1 mm²/s (data verified based on the calibration reports of the device) [16]. The density of individual samples in this experiment was determined in accordance with PN-EN ISO 12185:2002 [36] using a DMA 4500 density analyzer (from Anton Paar GmbH, Graz, Austria) with oscillating U-tube performing measurements. The accuracy of the temperature setting is 0.02 °C, while the accuracy of the density measurement is 5×10^{-5} g/cm³ [16].

2.4. Tribological Properties of the Lubricating Oil Diluted with Diesel Oil

Lubricity is a complex property of both oil and solids that operate under boundary friction conditions in the presence of oil. It characterizes the behavior of the lubricant during boundary friction [55]. It is a measure of the oil's ability to form a boundary layer as a result of physical and chemical adsorption [55]. Boundary layers ensure a reduction of friction resistance and protection against excessive wear of cooperating elements of friction pairs [16]. This is particularly important in relation to the tribological pairs that are characterized by low relative speeds of the cooperating elements, high loads, and high operating temperatures, such as the sliding bearings of marine engines [56].

Lubricity depends on the properties of the oil and the contacting materials, their surface condition, load, contact geometry, movement, and many other factors. Lubricity is approximated using tribometers (tribotesters [57] and methods for lubricating oils [58] and biofuels [59]), in which the destruction of the surface layer is performed in model-controlled conditions. One commonly recommended method for determining the lubricity of lubricating and diesel oils is to measure the multiplicity of the average diameter of the wear trace of a test piece; this is achieved using a High-Frequency Reciprocating Rig (HFFR). The method used, as an element for assessing the usability of the distillate fuels, is recommended by many standards, e.g., 450/2000 [60].

Measurements in this experiment were conducted with a tribometer model HFFR V1.0.3 (from PCS Instruments, London, UK). The device performed measurements in accordance with ASTM D 6079 [61] and PN-EN ISO 12156-1 [38]. The size of the wear mark was performed using a standard optical (metallurgical) microscope with vertical illumination HFR2 (from PCS Instruments, London, UK). Basic technical data relating to the set used in the experiment are presented in Appendix C.

A sample of the test liquid is positioned in the test reservoir at a specific temperature (here, according to ISO 12156-1 [38], this is 60 °C) determined by the bath. The HFFR apparatus uses a steel ball that is loaded against a stationary steel plate; it is fully submerged in the test liquid. The load provided in the device is 200 g. During the lubricity measurement, the ball is positioned into high-frequency oscillations, while maintaining constant contact with the steel plate. The schematic diagram of the device is shown in Figure 2.

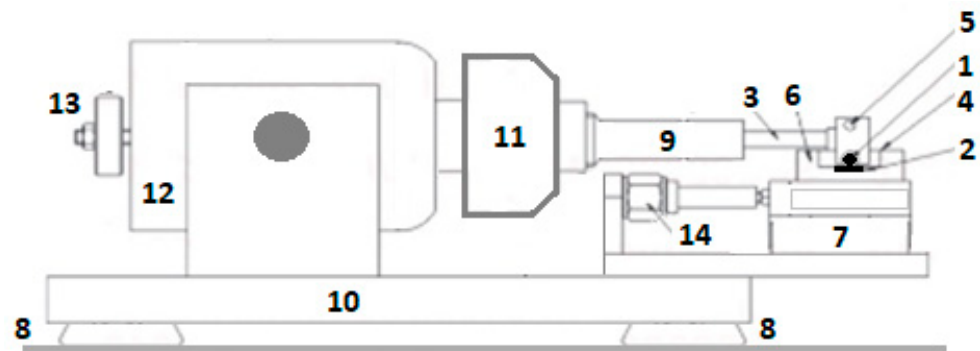


Figure 2. Schematic of the HFFR apparatus (own elaboration): 1—test ball, 2—test plate, 3—oscillating rod, 4—test fluid reservoir, 5—test mass, 6—heating bath, 7—support, 8—controllable base, 9—elastic lock, 10—main frame, 11—elastic connector housing, 12—electromagnetic vibrator, 13—counterweight, and 14—force transducer.

After the ball surface wear test, the diameter of the wear mark is measured in terms of a value that determines the lubricity of the tested lubricant under model conditions. Measurement of the size of the wear mark is performed using one of two methods, either using a digital camera or a visual observation. The details of the measurements are found in the dedicated ISO 12156-1:2018 standards [38] or ASTM D 6079 [61].

The uncorrected mean wear scar diameter WSD (μm) is defined as the mean value of the wear scar dimension x (μm) and y (μm) when measured perpendicular and parallel, respectively, to the direction of oscillation, so that:

$$WSD = \frac{x + y}{2}, \quad (12)$$

This value does not consider the temporary conditions in the laboratory; therefore, in practice, the corrected value $WS_{1.4}$ (μm) is used, which is defined at a pressure $p = 1.4$ kPa [62]. The $WS_{1.4}$ parameter is a standard measure of the lubricity used in the description of diesel fuel systems [55].

To determine the value of $WS_{1.4}$, in addition to finding the size of the wear trace WSD , it is also necessary to measure the temperature t_1 (°C) and humidity h_1 (%) of the air in the laboratory room at the beginning of each testing procedure and the temperature t_2 (°C) and humidity h_2 (%) of the atmosphere at its conclusion. The absolute vapor pressures at the beginning of the test, AVP_1 (kPa), and the absolute vapor pressures at the end of the test, AVP_2 , are determined according to the following formulas [63]:

$$AVP_1 = \frac{h_1 \cdot 10^{\frac{8.017352 - \frac{1705.984}{231.864 + t_1}}}{750}}, \quad (13)$$

$$AVP_2 = \frac{h_2 \cdot 10^{8.017352 - \frac{1705.984}{231.864 + t_2}}}{750}, \quad (14)$$

The parameters AVP_1 and AVP_2 are used to calculate the average absolute vapor pressure during the AVP test (kPa) as a result of the arithmetic mean, meaning that:

$$AVP = \frac{AVP_1 + AVP_2}{2}. \quad (15)$$

The final corrected value of the wear trace (lubricity) $WS_{1.4}$ is calculated according to the following relationship [63]:

$$WS_{1.4} = WSD + HCF \cdot (p_r - AVP), \quad (16)$$

where p_r denotes the reference pressure equal to 1.4 kPa and HCF is the proportionality factor equal to $60 \frac{\mu m}{kPa}$ for unknown fuel samples. The required measurement accuracy is indicated in the mentioned standards. Accuracy is determined by repeatability, i.e., two test results obtained by the same operator with identical apparatus under constant operating conditions acting on identical test materials produce the same result. Reproduction would also be required for two single and independent results obtained by different operators working in different laboratories on identical test materials.

The repeatability for measuring liquids at 60 °C in accordance with ASTM D 6079 [61] is 80 μm and for ISO 12156-1 [38] it is 50 μm , when using the digital camera method and 70 μm for the visual observation procedure. Moreover, the reproducibility for the measurements of the liquids at a temperature of 60 °C in accordance with the ASTM D 6079 standard [61] is 136 μm , while for ISO 12156-1 [38] it is 80 μm for the digital camera method and 90 μm for the visual observation procedure. The process in this test method has no bias because the lubricant is not fundamental and does not have the properties of the test liquid and, thus, it is evaluated in terms of this test method [61]. With this in mind, it can be assumed that this experiment (for the measurement of lubricity) requires a repeatability of $\geq 50 \mu m$ and a reproducibility of $\geq 80 \mu m$.

The HFFR apparatus, in addition to measuring the $WS_{1.4}$ value, enables the determination of the average value of the sliding friction coefficient μ and the $FILM$ parameter, which describes the reduction in percentage for oil film resistance during the test. The coefficient of sliding friction for the kinetic friction is the ratio of the friction force F to the force P of the body on the ground (i.e., another body) during the mutual sliding motion of these bodies, i.e., Equation (5).

The values of the friction coefficient strongly depend on the type of cooperating surfaces (materials, processing, etc.), the substance separating them (the lubricating oil in this case), and the impurities between the cooperating bodies and many other factors. The thickness of the oil film and its quality is found using the $FILM$ parameter, which is determined by the electrical contact potential (ECP) measurement. This is a measure of the contact resistance (i.e., the oil film resistance). The contact resistance circuit in the employed device applies a potential of 15 mV to the stabilizing resistor with a default resistance value of 10 Ω and a series sample contact resistor. The stabilizing resistance is set by the control software. The HFFR apparatus, after the test, provides the value of the percentage reduction in the oil film resistance value according to the relationship:

$$FILM = \frac{R_1 - R_2}{R_1} \cdot 100 = \frac{|U_1 - U_2|}{U_1} \cdot 100, \quad (17)$$

where R_1 (Ω) and R_2 (Ω) are the oil film resistance values at the beginning and end of the oil lubricity test, respectively, and U_1 (mV) and U_2 (mV) are the contact potential values at the beginning and end of the oil lubricity test, respectively.

A decrease in the $FILM$ parameter to a value that is equal to or close to zero indicates the existence of metallic contact (i.e., oil film breakage) between the sliding surfaces. In

addition, large values for the *FILM* parameter indicate a separation of the cooperating metal surfaces [16].

3. Results and Discussion

3.1. Ignition Properties of Oil Diluted with Diesel Oil

The change in the value of the ignition temperature, alongside the change in the composition of the mixture of lubricating oil and diesel oil, is shown in Figure 3. For both tested lubricating oils, there is a direct relationship between the content of the diesel oil in the mixture with lubricating oil and the flash point temperature. As the diesel oil content in the mixture increases, the flash point decreases from approximately 180 °C for the pure lubricating oil to 62.5 °C for 75% m/m diesel oil mixed with lubricating oil. In addition, for both mixtures, a similar dependence on the effect of diesel oil in a mixture with lubricating oil on the flash point temperature can be observed. The highest decrease in the flash point temperature for both mixtures (by approximately 59%) can be observed in the first section of the curve for the content of approximately 10% m/m of diesel oil in the mixtures, with the additional part of the curves characterized by a slight smoothing. The content of 30% m/m for the diesel oil in the mixture causes the flash point temperature to drop by as much as 85% compared to pure lubricating oils.

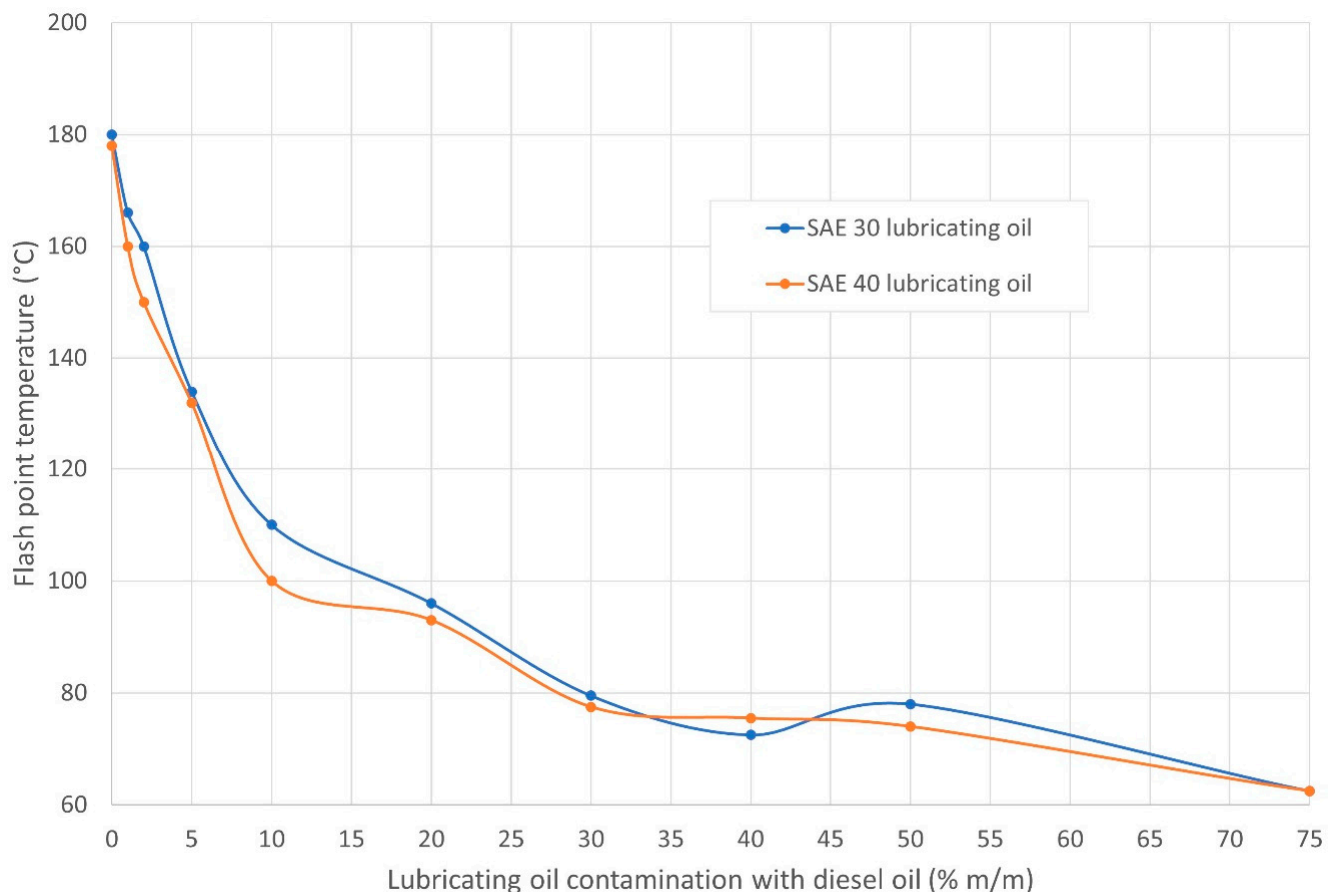


Figure 3. Flash point temperature values as a function of mass fraction of the diesel oil in the tested mixtures of lubricating oil and diesel oil.

Pearson's correlation coefficient values for the measurements of ignition temperatures and diesel oil content in the tested mixtures were $r_{XY} = -0.870$ for the SAE 30 oils and $r_{XY} = -0.850$ for the SAE 40 oils. In both cases, a very large negative correlation arose that represents a very high dependence on the analyzed variables.

The values of the calculated cetane index, as a function of changing the composition of the mixture of lubricating oil and diesel oil, are shown in Figure 4. For the SAE 30 oils,

the lowest concentration of diesel oil in a mixture with lubricating oil (for which tests were possible) is 30% m/m diesel oil for the SAE 30 viscosity grade oil mixtures and 40% m/m diesel oil for SAE 40. For both tested lubricating oils, there are slight fluctuations in the CCI values, i.e., in the range of 47.8–52.4 for the SAE 30 oil mixtures and 49.2–52.1 for the SAE 40 oil mixtures. It can therefore be assumed that the changes in the auto-ignition delay in the analyzed range of the diesel oil concentrations in the tested mixtures are insignificant, and that all the tested mixtures are characterized by excellent ignition properties.

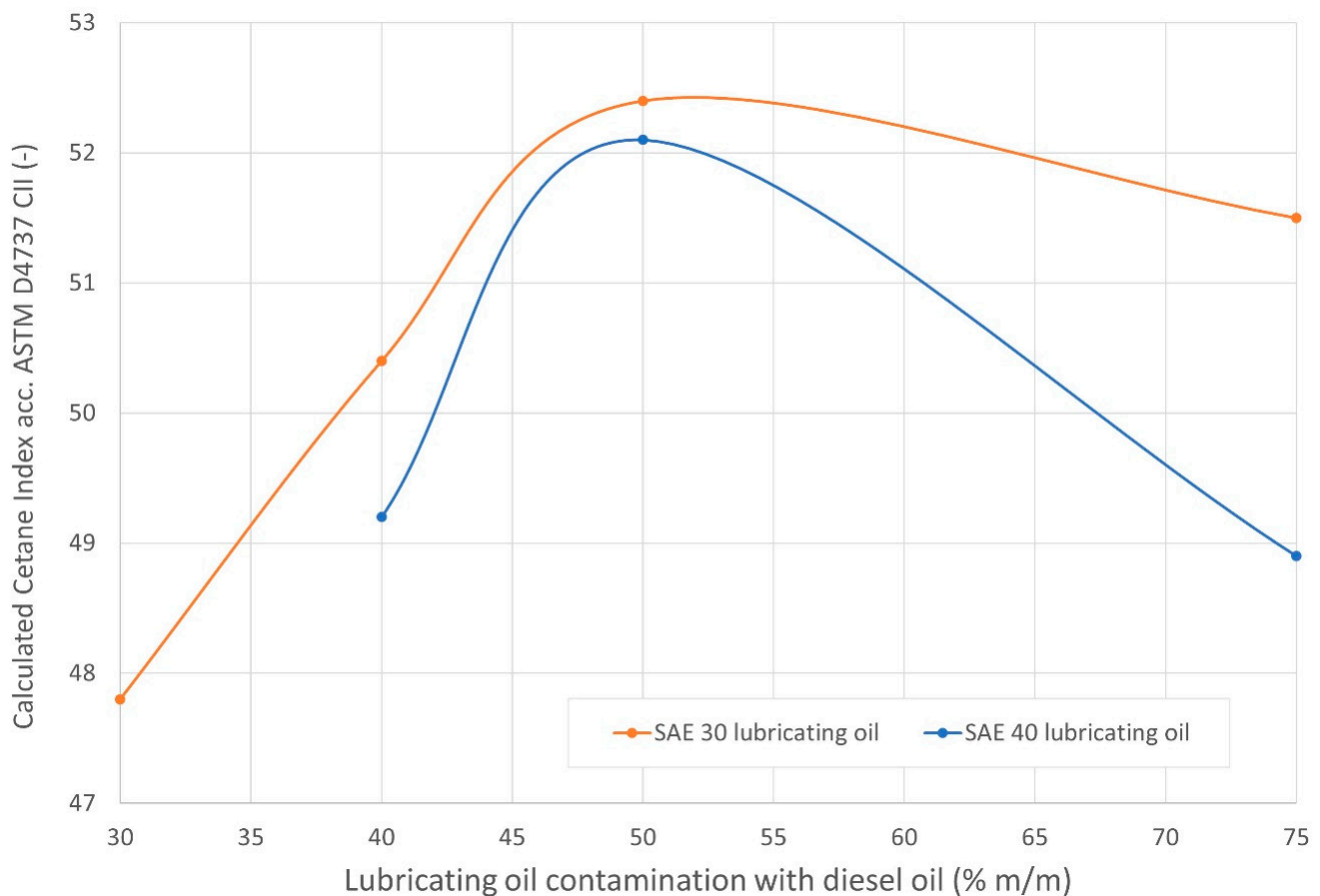


Figure 4. Calculated cetane index (in accordance with the ASTM D4737-21) as a function of the mass fraction of diesel oil in the tested mixtures of the lubricating oil and diesel oil.

The confirmation of the lack of a visible functional relationship between the obtained CCI values and the diesel oil content in the tested mixtures with lubricating oils arose due to the large discrepancies in the values of Pearson's correlation coefficient for these variables, namely, $r_{XY} = 0.694$ for the mixtures of lubricating oil of viscosity grade SAE 30 and $r_{XY} = -0.322$ for SAE 40.

Thus, in accordance with the previously adopted criteria for assessing the correlation, there is a highly positive correlation for the mixtures of SAE 30 lubricating oil and a low negative correlation for SAE 40. The reason for this outcome is the small number of measurement points for the tested indicator (i.e., 4 points for SAE 30 oil mixtures and 3 points for SAE 40 oil mixtures) and the small differences in the value of the $\Delta CCI < 5$ index in the entire analyzed range of the diesel oil concentration variability, from 30% m/m diesel oil in mixtures with SAE 30 and 40% m/m with SAE 40 to 75% m/m diesel oil in the mixture with lubricating oil.

3.2. Rheological Properties of the Lubricating Oil Diluted with Diesel Oil

The basic rheological index that is found during the experiment is the dynamic viscosity, which is determined based on the measurement of the kinematic viscosity and density. To discover the variability of these parameters with a change in the temperature, the viscosity index is additionally determined based on the values of kinematic viscosity at 40 °C and 100 °C, and the coefficient of temperature density change found for the density of the tested mixtures at 15 °C and 100 °C.

Figure 5 depicts the density values of the mixtures of SAE 30 and SAE 40 lubricating oils with diesel oil, which depend on the mass concentration of the diesel oil in these mixtures. The density values are measured at a standard temperature of 15 °C and the reference temperatures for dynamic viscosity values of 40 °C and 100 °C. All the characteristics show the nature of the relationships as a function of the concentration of the tested mixture. According to the properties of lubricating oils and fuels, the density decreases with increasing temperature. The characteristics of the mixtures of SAE 30 and SAE 40 lubricating oil are very similar; the difference in the density values between these mixtures at a given measurement temperature and for a given concentration (for the tested ranges) does not exceed 3.16 kg/m³. This applies to mixtures with a content of diesel oil in a mixture with lubricating oil of 75% m/m at a temperature of 40 °C.

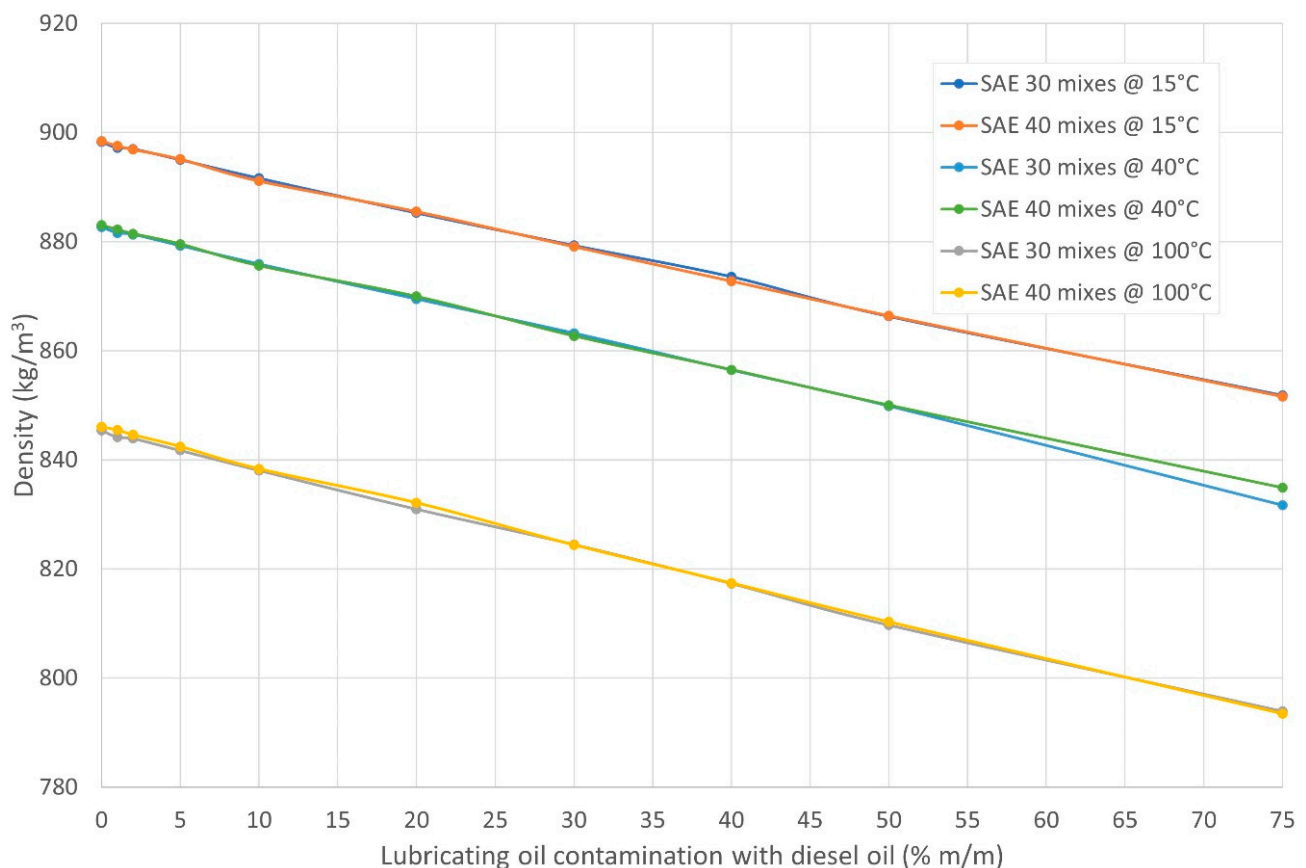


Figure 5. Density values of the tested mixtures of the lubricating oil and diesel oil as a function of the mass fraction of the diesel oil in the tested mixtures of the lubricating oil and diesel oil at measurement temperatures of 15 °C, 40 °C, and 100 °C.

Pearson's correlation coefficient values for the measurements of the density and the diesel oil content in the tested mixtures for all three measurement temperatures were $r_{XY} = -1.000$. Thus, in all six cases, a very high negative correlation occurred, which, in the case of such a high absolute value of r_{XY} , should be interpreted as a complete relationship.

The values of the coefficient of temperature density change ε determined for the density at 15 °C and 100 °C of the tested mixtures of lubricating oil and diesel oil, as a function of the mass concentration of diesel oil in the mixture, are presented in Figure 6. The coefficient ε quantifies the decrease in the density of the mixture when heated by 1 °C. For both mixtures of the lubricating oils for the SAE 30 and SAE 40 grades, an increase in the value of the coefficient is observed in the range between 0.61 and 0.69 kg/(m³·K) as a function of the rise in the content of the diesel oil in the mixture with the lubricating oil. The values of coefficient ε for both mixtures are similar, while the addition of 10% m/m of diesel oil in the mixture causes an increase of this factor by approximately 15% and for the addition of 30% m/m, this factor is escalated by approximately 38% compared to the pure lubricating oil (for SAE 30 or SAE 40).

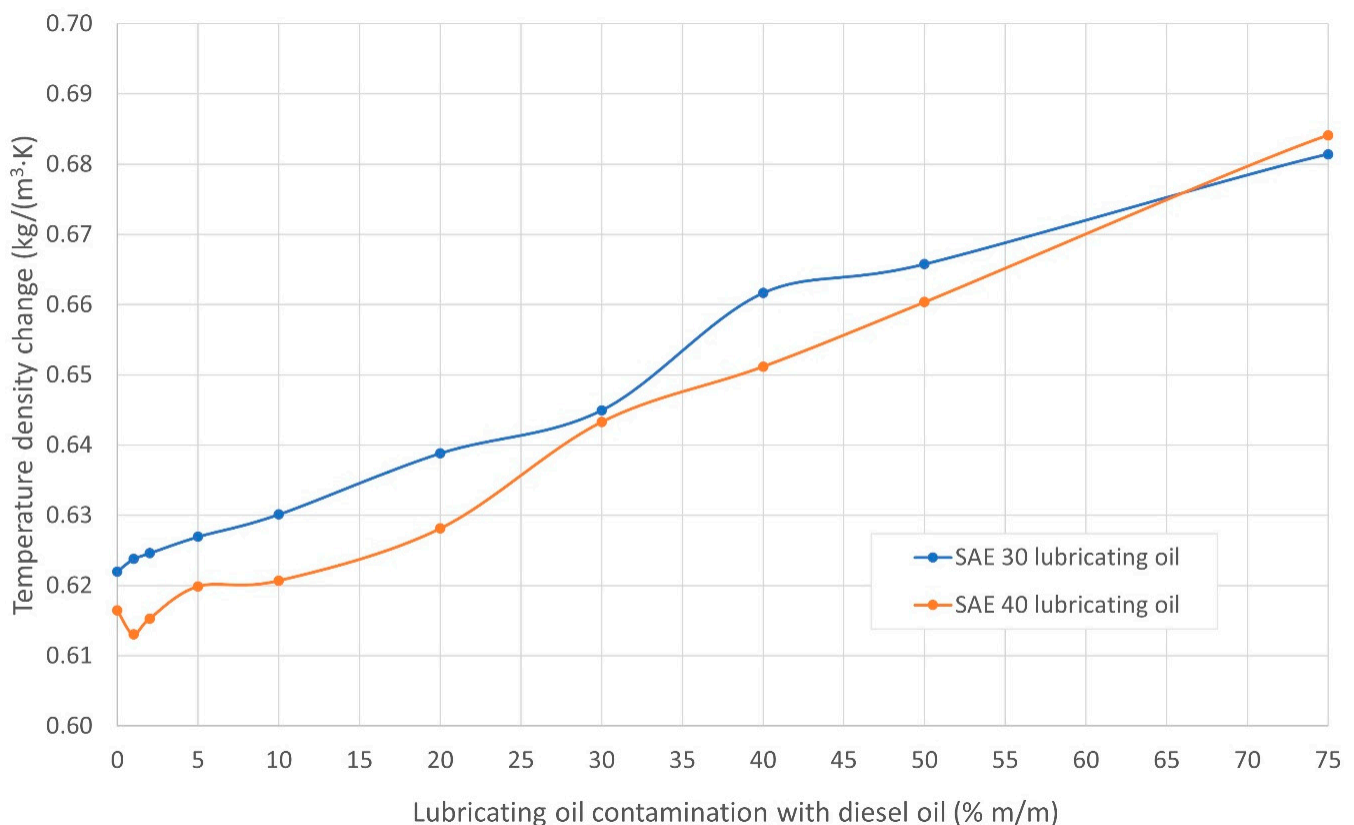


Figure 6. Values of the temperature density change for the temperature range of 15–100 °C of the tested mixtures of the lubricating oil and diesel oil as a function of the mass share of the diesel oil in the tested mixtures of the lubricating oil and diesel oil.

Pearson's correlation coefficient values for the determined values of the ε coefficient and the diesel oil content in the tested mixtures were $r_{XY} = 0.993$ for SAE 30 lubricating oil mixtures and $r_{XY} = 0.996$ for SAE 40. In both cases, a very high positive correlation arose. Here, an increase in the diesel oil content in the mixture resulted in an increase in the ε coefficient, which, in the case of such a high value, should be interpreted as a very high-to-full dependence.

Figure 7 depicts the values of the kinematic viscosity ν of the mixtures of SAE 30 and SAE 40 lubricating oils with diesel oil, which depend on the mass concentration of the diesel oil in these mixtures. The values of ν are measured at the standard temperatures of 40 °C and 100 °C. All the characteristics show the nature of the relationships as a function of the concentration of the tested mixture. According to the properties of lubricating oils and fuels, the kinematic viscosity decreases with increasing temperature. At 40 °C, the kinematic viscosity of the SAE 30 lubricating oil mixtures decreases from ~105 mm²/s to ~5 mm²/s, and for the SAE 40 oil mixtures, from ~160 mm²/s to ~6 mm²/s, which is a

decrease in kinematic viscosity of almost 95% in both cases. At 100 °C, the viscosity of the SAE 30 lubricating oil mixtures decreases from $\sim 12 \text{ mm}^2/\text{s}$ to $\sim 2 \text{ mm}^2/\text{s}$, and for SAE 40 oil mixtures, from $\sim 15 \text{ mm}^2/\text{s}$ to $\sim 2 \text{ mm}^2/\text{s}$.

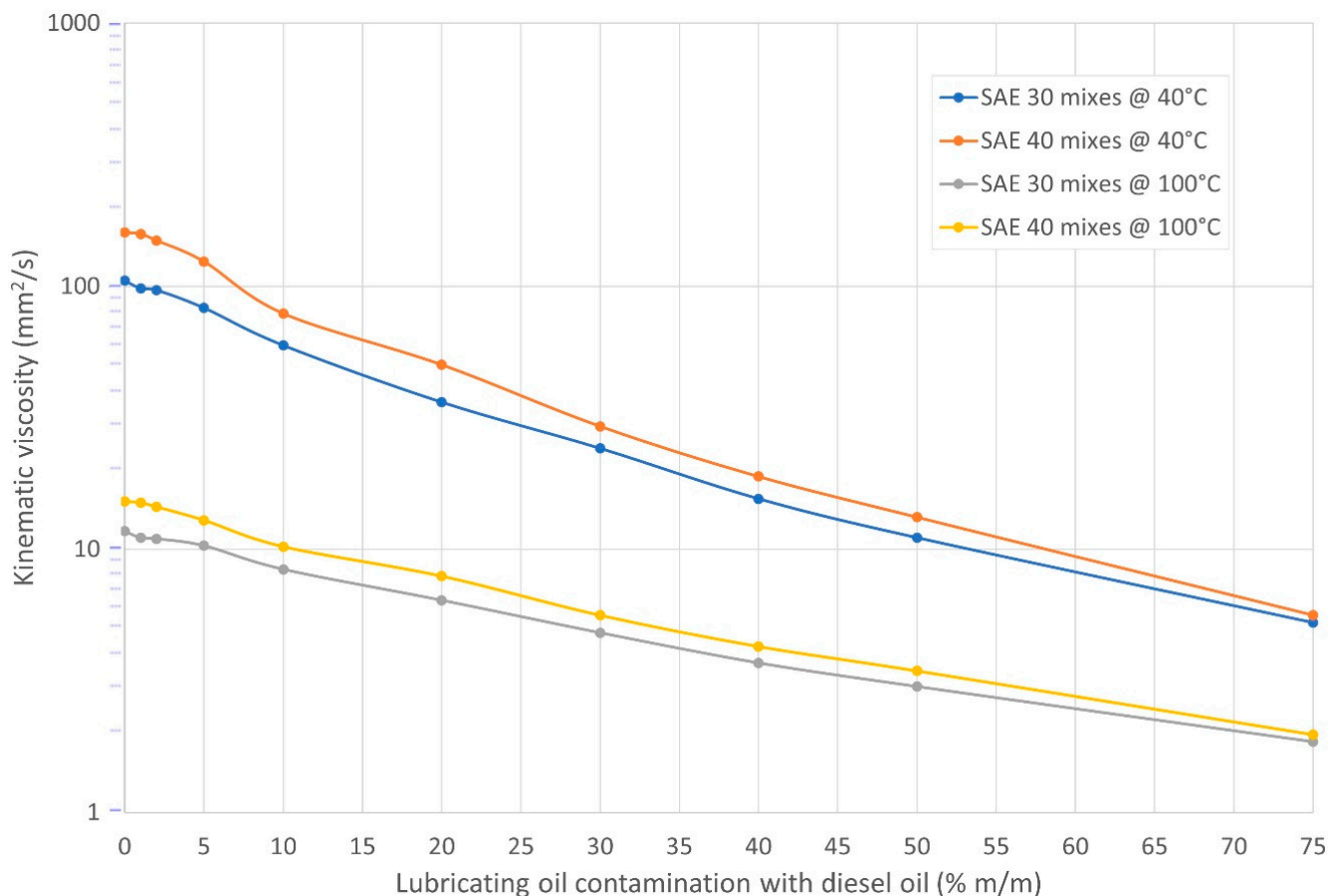


Figure 7. Values of the kinematic viscosity of the tested mixtures of the lubricating oil and diesel oil as a function of the mass fraction of the diesel oil in the tested mixtures of the lubricating oil and diesel oil at measurement temperatures of 40 °C and 100 °C.

Pearson's correlation coefficient values for the measured values of the kinematic viscosity ν and the diesel oil content in the tested mixtures were (for measurements at 40 °C) $r_{XY} = -0.904$ for the SAE 30 lubricating oil mixtures and $r_{XY} = -0.884$ for SAE 40. However, for measurements at 100 °C, $r_{XY} = -0.950$ for SAE 30 and $r_{XY} = -0.940$ for SAE 40 were determined, which denote very high negative correlations (i.e., an increase in the diesel oil content in the mixture results in a decrease in kinematic viscosity, which, in the case of such a high absolute value of r_{XY} , should be interpreted as a very strong relationship).

Figure 8 displays the values of the dynamic viscosity η of the mixtures of SAE 30 and SAE 40 lubricating oils with diesel oil, which depend on the mass concentration of the diesel oil in these mixtures. The η values are measured at the standard temperatures of 40 °C and 100 °C. All the characteristics show a linear relationship as a function of the concentration of the tested mixture, which results from the analogous relationships and the nature of changes for the density and the kinematic viscosity. According to the properties of the lubricating oils and fuels, the dynamic viscosity decreases with increasing temperature. At 40 °C, the viscosity of the SAE 30 lubricating oil mixtures decreases from $\sim 93 \text{ mPa}\cdot\text{s}$ to $\sim 2 \text{ mPa}\cdot\text{s}$, and for SAE 40, from $\sim 141 \text{ mPa}\cdot\text{s}$ to $\sim 5 \text{ mPa}\cdot\text{s}$. However, at 100 °C, the viscosity of the SAE 30 lubricating oil mixtures decreases from $\sim 10 \text{ mPa}\cdot\text{s}$ to $\sim 1 \text{ mPa}\cdot\text{s}$, and for SAE 40, from $\sim 13 \text{ mPa}\cdot\text{s}$ to $\sim 1 \text{ mPa}\cdot\text{s}$.

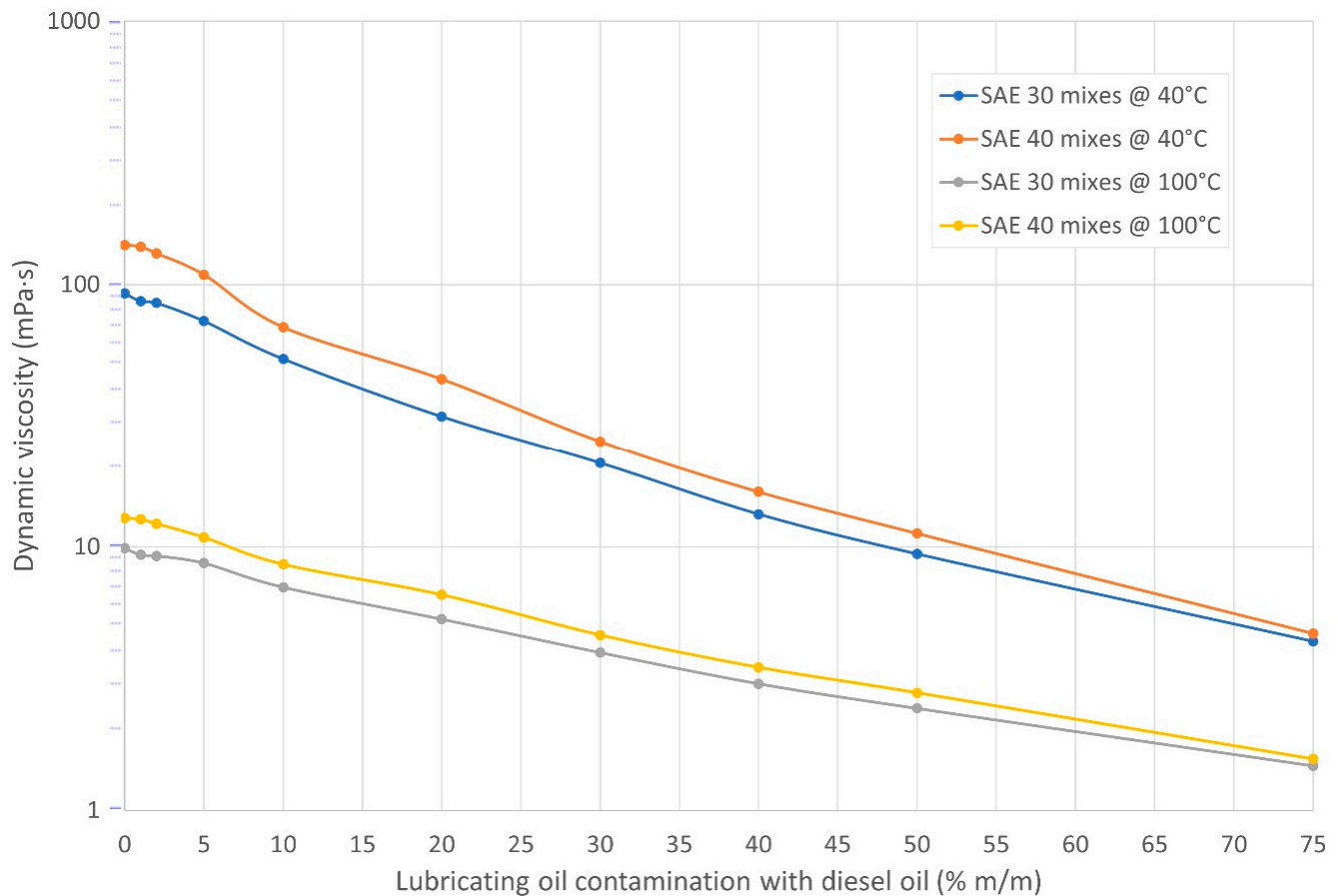


Figure 8. Dynamic viscosity values of the tested mixtures of the lubricating oil and diesel oil as a function of the mass fraction of the diesel oil in the tested mixtures of the lubricating oil and diesel oil at measurement temperatures of 40 °C and 100 °C.

Pearson's correlation coefficient values for the measured values of the dynamic viscosity η and the diesel oil content in the tested mixtures were $r_{XY} = -0.903$ for SAE 30 and $r_{XY} = -0.883$ for SAE 40 when taking measurements at 40 °C. However, for measurements at 100 °C, $r_{XY} = -0.948$ for SAE 30 and $r_{XY} = -0.937$ for SAE 40. In the four cases, a very high negative correlation arose (i.e., an increase in the diesel oil content in the mixture results in a decrease in kinematic viscosity, which, in the case of such a high absolute value of r_{XY} , should be interpreted as a very strong relationship).

Based on the kinematic viscosity values at 40 °C and 100 °C of the tested mixtures of the lubricating oil and diesel oil, the viscosity index VI is calculated. The values of this indicator, as a function of the mass concentration of diesel oil in the mixtures, are shown in Figure 9. The viscosity index is a measure of a fluid's change in viscosity relative to the temperature change. The lower the viscosity index VI, the more the viscosity is modified with the temperature change (i.e., it decreases with a temperature increase). For both mixtures of the tested lubricating oils of SAE 30 and SAE 40 grades, an increase in the viscosity index in the range between ~95 and ~160 is observed as a function of the rise in the diesel oil content in the mixture with the lubricating oil.

Pearson's correlation coefficient values for the determined values of the viscosity index VI and the diesel oil content in the tested mixtures were $r_{XY} = 0.948$ for SAE 30 and $r_{XY} = 0.970$ for SAE 40. In both cases, a very high positive correlation arose (i.e., an increase in the diesel oil content in the mixture results in an increase in the viscosity index VI value, which, in the case of such a high value, should be interpreted as a very strong relationship).

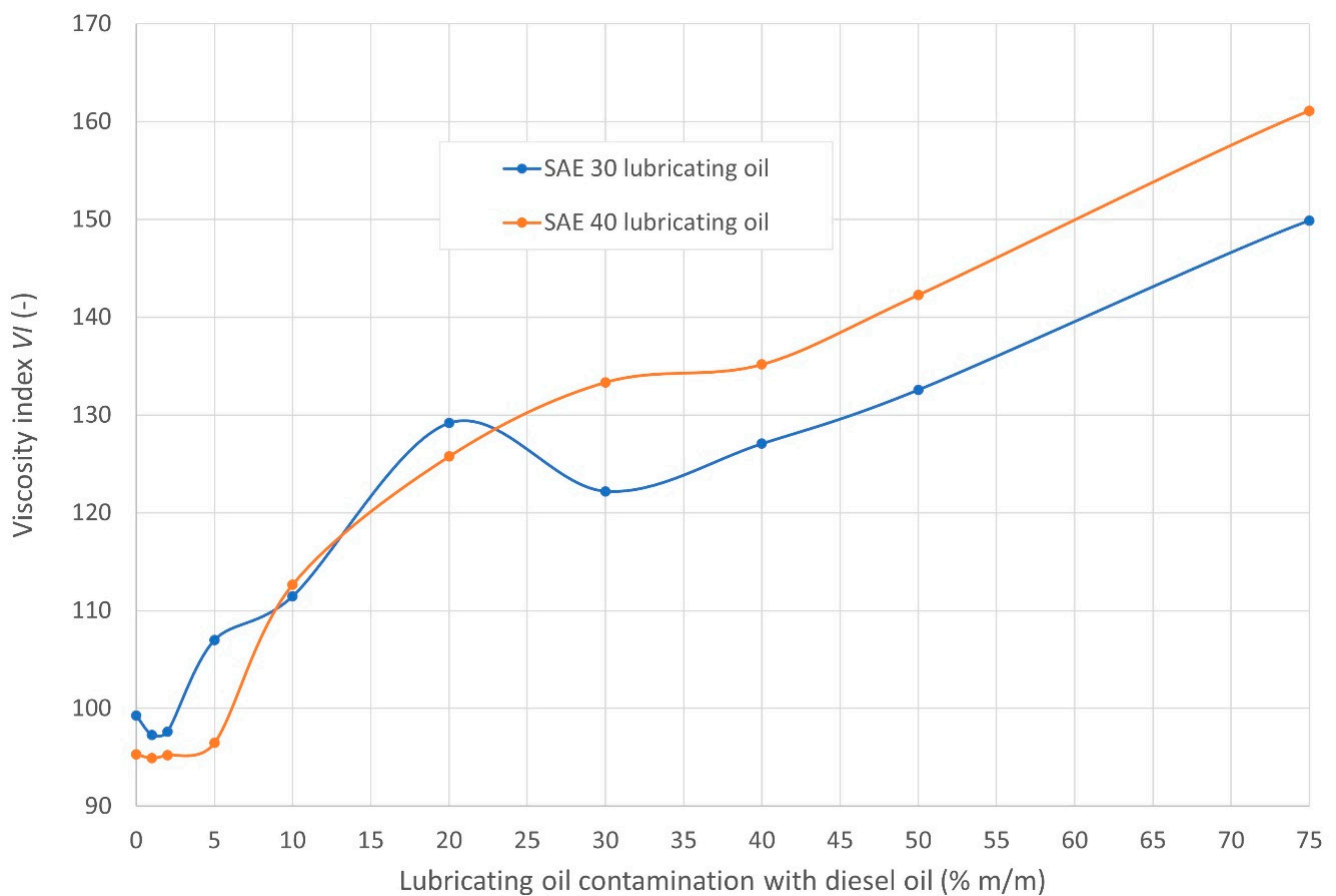


Figure 9. Viscosity index VI values of the tested mixtures of the lubricating oil and diesel oil as a function of the mass share of the diesel oil in the tested mixtures of the lubricating oil and diesel oil.

3.3. Tribological Properties of the Lubricating Oil Diluted with Diesel Oil

The values of the parameters that describe lubricity as a function of diesel oil concentration in the tested mixtures of the lubricating oils and the diesel oil for mixtures of SAE 30 and SAE 40 lubricating oil are shown in Figures 10 and 11, respectively. Among the analyzed parameters obtained at the HFFR station, the maximum value of the wear trace in the direction parallel and perpendicular to the axis of the arm of the HFFR apparatus (moving the sample in the x - and y -directions) is recorded, as well as the average wear trace WSD and the normalized wear trace $WS_{1.4}$. Example wear traces obtained during the tests are shown in Figure 12.

For the mixtures of both tested lubricating oils, the fluctuations of the values of all the listed indicators that describe lubricity are visible. There is no clear trend for the changes, and the lubricity values undergo changes of a relatively complex nature (i.e., periodic increases and decreases in the values of the parameters describing lubricity). For mixtures of diesel oil and lubricating oil SAE 30, these values range from 69 to 339 μm , and for SAE 40, it is in the range of 89–245 μm .

The values of the maximum deviation of the lubricity, from the respective average values, are close to the previously indicated values for repeatability and reproducibility. The latter makes it possible to claim that the tiny differences in the lubricating properties of the lubricating oils of the tested grades and the diesel oil are so slight that they cannot be recorded and, thus, note the effect of the contamination of the lubricating oil with the diesel oil on the deterioration of the lubricity of the cooperating elements of the tribological pair separated by this oil acting as a lubricant.

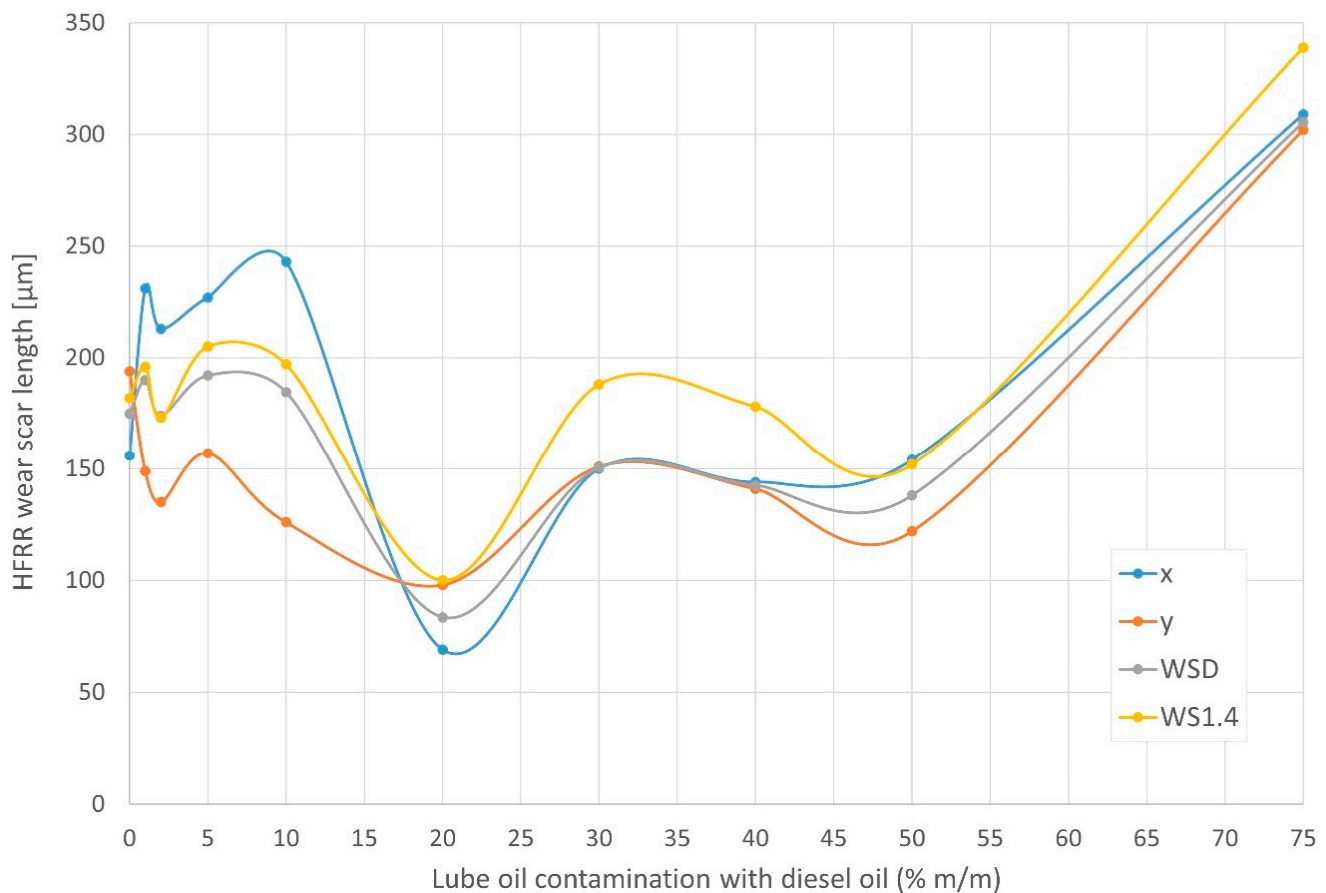


Figure 10. HFRR lubricant test results as a function of the diesel oil mass fraction in the tested mixtures of the SAE 30 lubricating oil and diesel oil.

The confirmation of the lack of a visible functional relationship between the obtained values of lubricity and the content of the diesel oil in the tested mixtures with lubricating oils relates to the discrepancies in the values of Pearson's correlation coefficient for these variables and their relatively low values. For mixtures of SAE 30 viscosity grade lubricating oil, the Pearson factors were $r_{XY} = 0.166$ for x , $r_{XY} = 0.517$ for y , $r_{XY} = 0.357$ for WSD , and $r_{XY} = 0.500$ for $WS_{1.4}$, which corresponds to a very low-to-moderate correlation. Moreover, for SAE 40, the Pearson coefficients were $r_{XY} = 0.034$ for x , $r_{XY} = 0.550$ for y , $r_{XY} = 0.265$ for WSD , and $r_{XY} = 0.617$ for $WS_{1.4}$, which corresponds to a very low-to-moderate correlation to moderate/high.

The large discrepancy between these values, and the fact that half of the indices are less than or equal to 0.500, proves that there is no clear trend for the changes. The latter may indicate that lubricity is maintained at an approximately constant level, regardless of the composition of the mixtures analyzed in the experiment.

The values of the mean coefficient of friction μ , as a function of the mass concentration of diesel oil in mixtures during the lubricity tests at the HFRR stand, are shown in Figure 13. The coefficient of sliding friction is a measure of the ratio of the friction force to the pressure force between the two cooperating (contacting) bodies in the mutual translational motion. An increase in the coefficient of friction indicates a growth in the value of the friction force [64]. In turn, the increase in these forces causes a growth in the temperature at the interface of the cooperating bodies [65]. The local temperature rises within the crankcase are referred to as hot spots; they are one of the elements of the oil mist formation [23] in the crankcase space that, when concentrated inside an explosive area, may explode when in contact with the elements when temperatures exceed the ignition temperature [66].

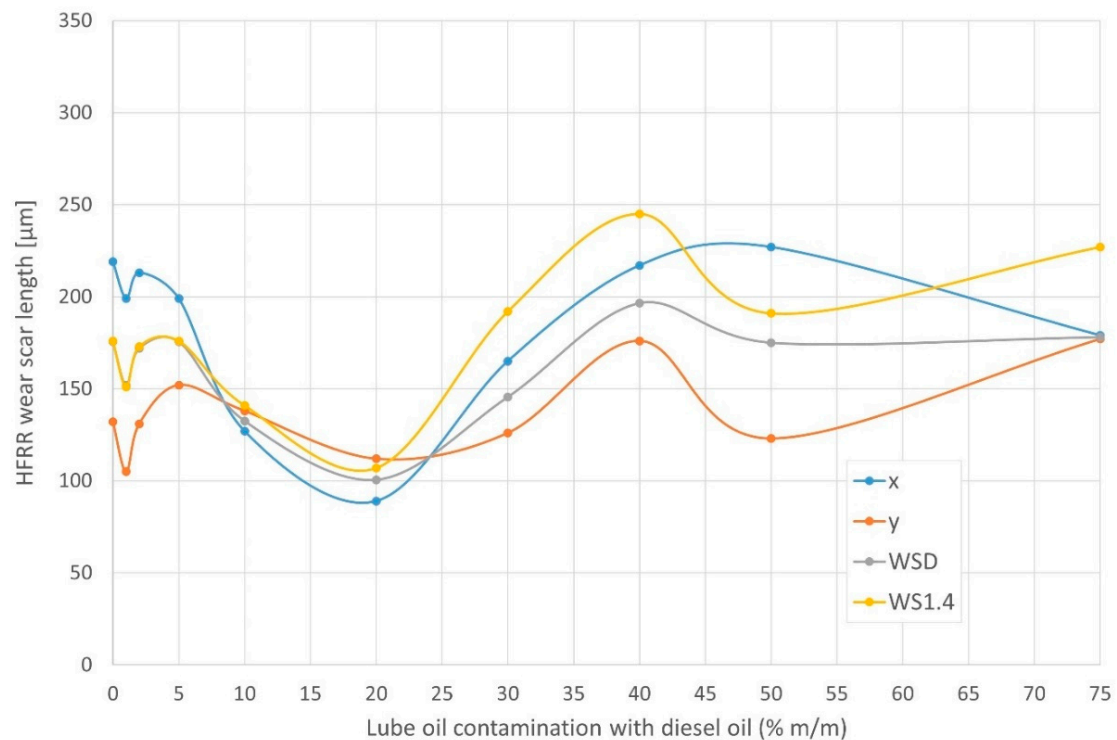


Figure 11. HFRR lubricant test results as a function of the diesel oil mass fraction in the tested mixtures of the SAE 40 lubricating oil and diesel oil.

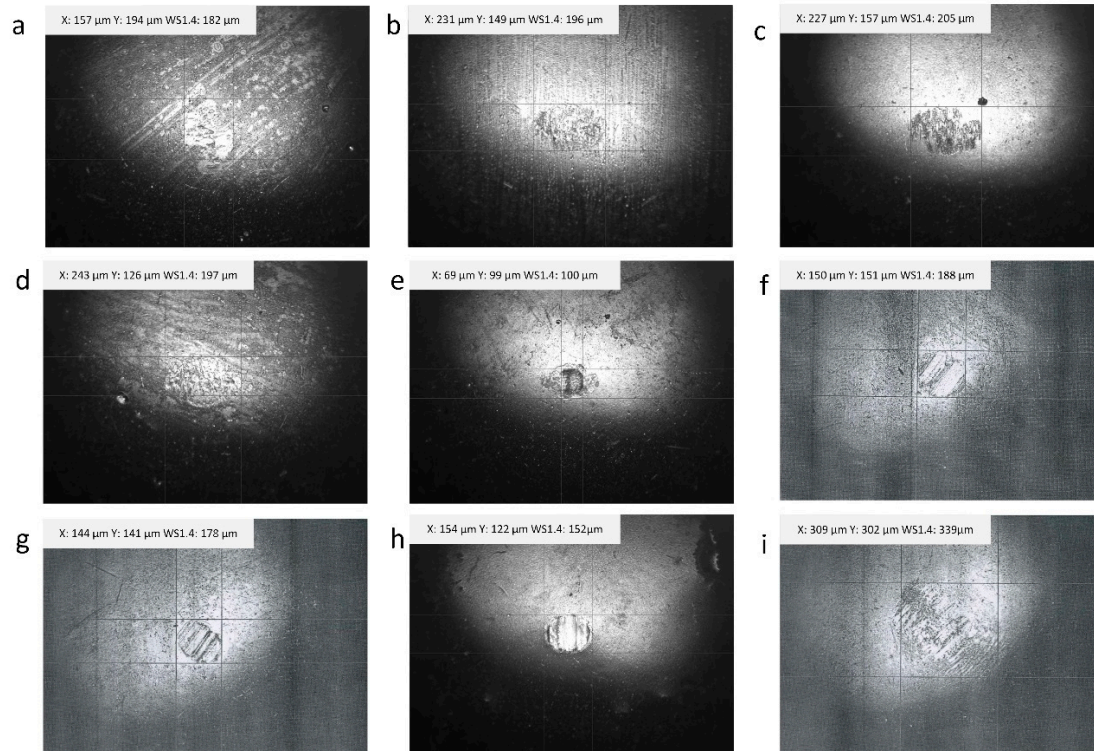


Figure 12. Selected photographs of traces of wear on a moving component after an HFRR lubricity test of SAE 30 lubricating oil mixes: (a) 100% SAE 30, (b) 99% m/m SAE 30 + 1% m/m DO, (c) 95% m/m SAE 30 + 5% DO, (d) 90 m/m SAE 30 + 10% m/m DO, (e) 80% m/m SAE 30 + 20% m/m DO, (f) 70% m/m SAE 30 + 30% m/m DO, (g) 60% m/m SAE 30 + 40% m/m DO, (h) 50% m/m SAE 30 + 50% m/m DO, (i) 25% m/m SAE 30 + 75% m/m DO.

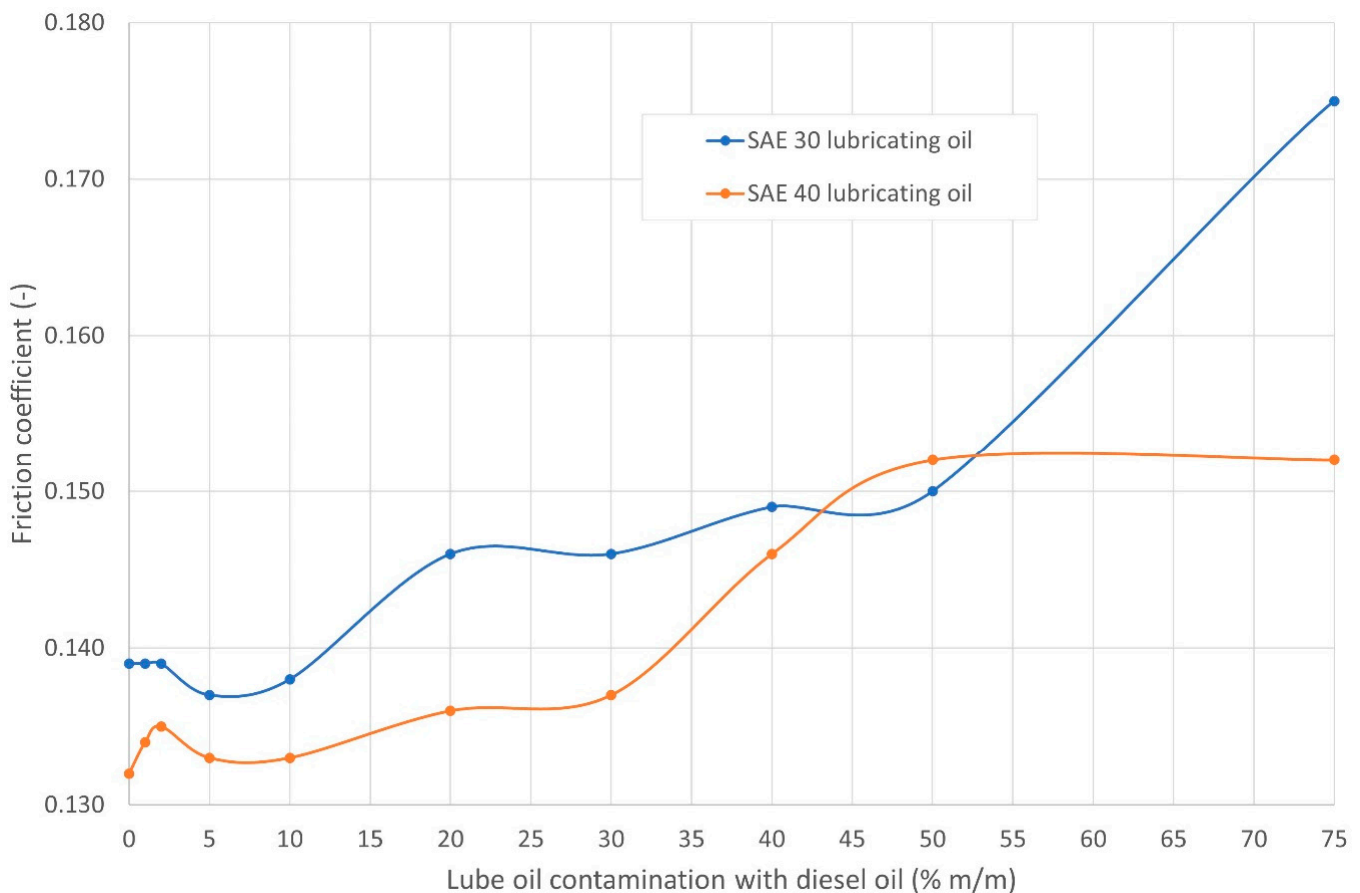


Figure 13. Mean coefficient of friction during the HFFR lubricity tests as a function of the diesel oil mass fraction in the tested mixtures with SAE 30 and SAE 40 lubricating oil.

For both mixtures of the tested lubricating oils with SAE 30 and SAE 40 grades, an increase in the value of the average coefficient of friction between the samples (separated by these mixtures during the lubricity test at the HFFR stand) is observed. These values increase as a function of the growth in the diesel oil content in the mixture with the lubricating oil in the range between 0.139 and 0.175 for mixtures of SAE 30 and between 0.132 and 0.152 for SAE 40. For both grades of lubricating oil that are contaminated with up to 10% m/m oil diesel, a slight change in the average friction coefficient (at approximately 1%) can be observed. However, for 30% m/m oil diesel in a mixture with a lubricating oil of SAE 30 grade and 40% m/m for SAE 40 grade, it significantly affects the average coefficient of friction, which causes increases of 5% and 11%, respectively.

Pearson's correlation coefficient values for the determined values of HFFR mean friction coefficient and the diesel oil content in the tested mixtures were $r_{XY} = 0.930$ for mixtures of SAE 30 lubricating oil and $r_{XY} = 0.940$ for SAE 40. In both cases, a very high positive correlation arose (i.e., an increase in the diesel oil content in the mixture results in an escalation in the μ value, which, in the case of such a high value, should be interpreted as a very strong relationship).

The last of the parameters analyzed is the percentage value of the *FILM* oil film resistance as a measure of the oil film thickness. The values of the *FILM* index, as a function of the mass concentration of the diesel oil in the mixtures during the lubricity tests at the HFFR stand, are shown in Figure 14. With a full separation of the samples that cooperate with the lubricant tested, the value of the *FILM* parameter is 100% and drops with a decrease in the thickness of the oil film. For both mixtures of the tested lubricating oils with SAE 30 and SAE 40 grades, a reduction in the value of the *FILM* parameter is observed for samples with increasing content of diesel oil in the tested mixture.

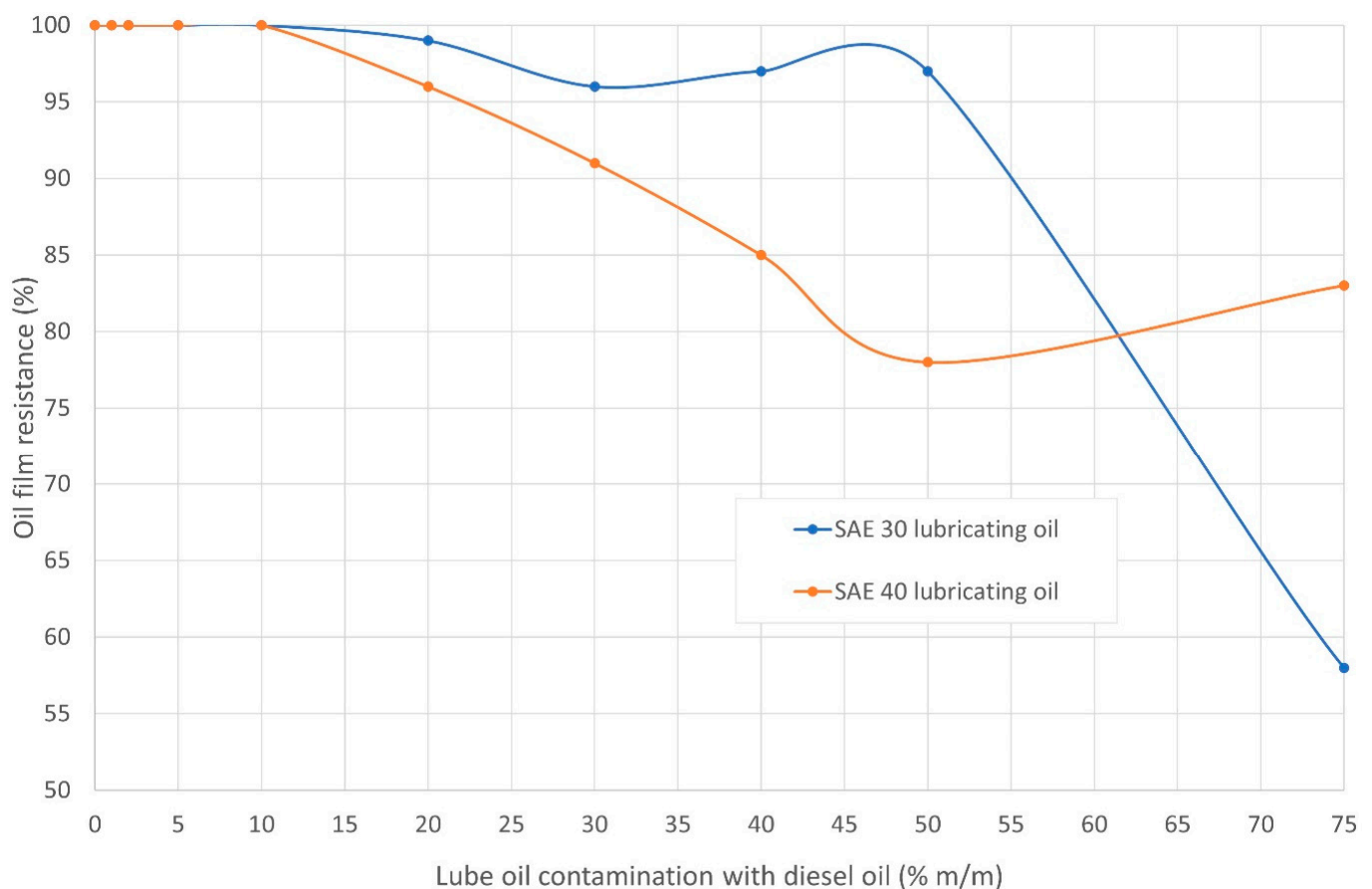


Figure 14. Oil film resistance during the HFFR lubricant tests as a function of the diesel oil mass fraction in the tested mixtures with SAE 30 and SAE 40 lubricating oil.

The values of the *FILM* parameter decrease as a function of the increase in the diesel oil content in the mixture with lubricating oil in the range between 100% and 58% for SAE 30 and between 100% and ~80% for SAE 40. Specifically, with the cooperation of the tested tribological pair at the HFFR stand and for samples separated by a mixture of SAE 30 lubricating oil and diesel oil, with the diesel oil content in the mixture equal to 75% m/m, the thickness of the oil film that separates the samples is reduced by 42% compared to the film thickness for the cooperating tribological pair that is separated by pure SAE 30 grade lubricating oil. However, with the cooperation of the tested tribological pair at the HFFR stand, and for samples separated by a mixture of SAE 40 lubricating oil and diesel oil, with the diesel oil content in the mixture equal to 75% m/m, the thickness of the oil film separating the samples is reduced by ~20% compared to the film thickness for the cooperating pair separated by a pure SAE 40 grade lubricating oil.

Pearson's correlation coefficient values for the determined values of the *FILM* parameter and the diesel oil content in the tested mixtures were $r_{XY} = -0.800$ for SAE 30 and $r_{XY} = -0.917$ for SAE 40. In both cases, a very high negative correlation occurred (i.e., an increase in the diesel oil content in the mixture results in a reduction in the value of the *FILM* parameter, which, in the case of such a high value, should be interpreted as a very strong relationship).

3.4. Aggregated Assessment of the Impact of Lubricating Oil Dilution with Distillation Fuel

Experimental studies of the effect of the distillation fuel on the ignition, rheological, and tribological properties (Table 6) of the lubricating oil diluted with this fuel showed that (in all the tested cases) no significant differences were found relating to the ability of the tested oil mixtures to create a boundary layer; the task of the latter is to reduce

friction resistance (Figures 10 and 11). However, with an increase in the concentration of the oil diesel in the tested mixtures of diesel and lubricating oils of SAE 30 and SAE 40 grades (Figure 14), a decrease in the thickness of the oil film and an increase in the coefficient of friction were observed. All the tested mixtures were characterized by very good ignition properties. Moreover, indices such as the flash point, density, kinematic, and dynamic viscosity showed a clear tendency to change with an increase in the dilution of the lubricating oil with diesel fuel. In addition, the change in temperature density and viscosity index increased with a growing dilution of the lubricating oil with the diesel oil.

Table 6. Evaluation of the correlation of the analyzed indicators for the composition of the tested mixture.

Properties	Parameter	Correlation with Diesel Oil Content in a Mixture with Viscosity-Grade Lubricating Oil		Comment
		SAE 30	SAE 40	
Ignition	Flash point temperature	Very high, negative	Very high, negative	Very high functional dependence. Flash point temperature decreases with increasing concentration of diesel oil in the tested mixture with lubricating oil.
	Calculated cetane number	High, positive	Low, negative	No apparent dependency. Observable slight fluctuations in value. All tested mixtures can be classified as fuels with very good ignition properties.
Rheological	Density	Very high, negative	Very high, negative	Very high-to-complete functional dependence. The density and viscosity of the mixtures decrease with increasing concentration of diesel oil in the tested mixture.
	Kinematic viscosity			
	Dynamic viscosity			
	Coefficient of temperature density change	Very high, positive	Very high, positive	Very high-to-full dependency. The coefficient of temperature change and the viscosity index increase with increasing concentration of diesel oil in the tested mixture.
	Viscosity index			
Tribological	Lubricity	Very low to moderate, positive	Very low to high, positive	No apparent dependency. Fluctuations in the values of parameters describing lubricity are observed. All tested mixtures can be classified as showing good lubricity.
	HFFR mean friction coefficient	Very high, positive	Very high, positive	Very high-to-full dependency. HFFR mean friction coefficient increases with increasing diesel oil concentration in the tested mixture.
	Relative thickness (resistance) of the oil film	Very high, negative	Very high, negative	Very high-to-full dependency. The relative thickness (resistance) of the oil film decreases with increasing concentration of diesel oil in the tested mixture.

The parameters that are used to quickly diagnose the contamination of the lubricating oil with diesel oil may include the ignition temperature, density, and viscosity (preferably at the same time to exclude other factors that cause changes in these parameters, such as oil contamination with water, wear products, the impact of bacteria and protozoa in the operating fluids, oil aging, etc.). The use of these parameters to assess the degree of dilution of the lubricating oil with the diesel oil provides the following relationships: an increase in the oil diesel content of the mixtures with lubricating oil results in a decreased ignition temperature (Figure 3), density (Figure 5), and viscosity (Figures 7 and 8).

4. Conclusions

Both in the case of SAE 30 and SAE 40 grade lubricating oil, diluting the lubricating oil with diesel fuel brings about a series of unfavorable changes, including a decrease in the thinning of the oil film and an increase in the coefficient of friction. In summary, based

on the obtained experimental results, it can be concluded that the critical contamination of oil with fuel in the range of 2–5% by weight, as indicated in the literature, still allows for a certain “safety margin”.

Nevertheless, it is recommended to take remedial action even in the case of low diesel oil concentration ($<5\%$ m/m) in the lubricating oil. This is confirmed by the fact that the tested oils did not meet the recommendations regarding their physical and chemical properties, such as the flash point already at the alarm level of dilution of lubricating oils with diesel oil equal to 1% m/m (a significant decrease below $180\text{ }^{\circ}\text{C}$ measured in a closed cup was observed) and kinematic viscosity at the alarm level of oil dilution lubricating oil equal to 5% m/m (a decrease in kinematic viscosity at $40\text{ }^{\circ}\text{C}$ greater than 20% compared to the value of fresh lubricating oil was observed).

If the concentration of diesel fuel in the lubricating oil exceeds $5\text{--}8\%$ m/m, the fuel contamination should be considered excessive and immediate remedial actions should be taken (such as fixing leakage sources and replacing/refreshing the oil). When the concentration of diesel fuel exceeds 10% m/m, there is a serious risk of engine damage during operation (a visible thinning of the oil film occurs).

Symptoms of lubricating oil dilution with diesel fuel include changes in viscosity and ignition temperature, and the causes of these symptoms should be diagnosed on a case-by-case basis. The conducted research indicates the need to monitor the content of diesel oil in the lubricating oil that, in the authors' opinion, could be a preventive measure against engine damage and should help ensure the reliable operation of the engine. This mainly applies to crosshead engines, in which there is a direct threat of fuel entering the engine crankcase. Especially significant is that the increasing value of the friction force (tested when determining the friction coefficient during the lubricity test of the tested mixtures of the diesel oil and lubricating oil) may contribute to the growth in the temperature of the lubricated elements. This contributes to the formation of an oil mist in the crankcase space. It may, therefore, cause an explosion in this system due to the abruptly increased temperature of the elements, which may exceed the ignition temperature of the mixture.

This research has shown no significant differences relating to the ability of the tested oil mixtures to create a boundary layer (lubricity). Moreover, the calculated cetane index has not changed significantly. Both can be associated with the content of biodiesel used and its complex composition, e.g., FAME have the ability to improve the lubricity of diesel oil.

Detailed research relating to various mixtures of oils with oil biodiesel blend impurities, and the increase in temperature caused by the tribological processes in the crankcase of a crosshead engine, will be the subject of further research by the authors. This future work will concern, among others, a determination of the aggregated indicators for the effects of dilution of the lubricating oil with diesel oil on the risk of engine damage or an explosion in the engine crankcase.

Author Contributions: Conceptualization, L.C.; methodology, L.C., P.K. and P.D.; software, L.C. and P.K.; validation, L.C., P.K. and P.D.; formal analysis, L.C., P.K. and P.D.; investigation, L.C., P.K. and P.D.; resources, L.C.; data curation, L.C.; writing—original draft preparation, L.C., P.K. and P.D.; writing—review and editing, L.C., P.K. and P.D.; visualization, L.C.; supervision, L.C.; project administration, L.C.; funding acquisition, L.C. All authors have read and agreed to the published version of the manuscript.

Funding: This research and the APC was funded by the Ministry of Science and Higher Education (MEiN) of Poland, grant number 1/S/KPBMiM/23. The APC was funded by MDPI.

Data Availability Statement: All data are available in this paper.

Acknowledgments: Laboratory tests were performed on behalf of the authors at the Center for Testing Fuels, Working Fluids, and Environmental Protection (CBPCRiOŚ) of the Maritime University of Szczecin. The authors would like to thank Magdalena Szmukała and Barbara Żurańska for their technical support and Katarzyna Gawdzińska for her advice.

Conflicts of Interest: The authors declare no conflict of interest. The funders had no role in the design of this study, in the collection, analysis, or interpretation of data, in the writing of this manuscript, or in the decision to publish the results.

Abbreviations

∇	vector differential operator (nabla)
A	heat transfer surface
$a_1, a_2, a_3,$ and a_4	proportionality factors
ASTM	ASTM International standard (formerly American Society for Testing and Materials)
AVP	mean absolute vapor pressure
AVP ₁	absolute vapor pressure at the beginning of the test
AVP ₂	absolute vapor pressure at the end of the test
CBPCRiOŚ	Center for Testing Fuels, Working Fluids, and Environmental Protection (pol. Centrum Badania Paliw, Cieczy Roboczych i Ochrony Środowiska)
CFR	Cooperative Fuels Research, manufacturer of test engines
CCI	calculated cetane index
C_m	average planning speed
DCN	derived cetane number measured (in accordance with the ASTM D 7668 standard [67])
d	wall thickness of the heat conductor
d_1	diameter of the cylinder liner on the warmer side
d_2	diameter of the cylinder liner on the cooler side
DO	diesel oil
ECN	estimated cetane number
F	sliding/friction force
FAME	fatty acid methyl esters
FILM	percentage drop in oil film resistance
HFFR	High-Frequency Reciprocating Rig
l	length (height) of the cylinder liner
P	pressure force, normal force between the object and the surface
p	unit pressure
p_r	reference pressure
R_1, R_2	oil film resistance at the beginning and end of the oil lubricity test
S_{gr}	product of planning speed and pressure values
T	absolute temperature
t	temperature measurement
∇T	temperature field gradient (grad T)
Δt	temperature difference on both sides of the heat conductor
t_0	temperature of the surface of the piston on the side of the exhaust gases
t_A, t_B	temperatures of surfaces A and B
t_{FP}	flash point temperature
T_R	friction force
t_{top}	material melting temperature
Q	thermal energy
\dot{Q}	heat stream
\dot{q}	unit heat stream of friction
U_1, U_2	electrical contact potential at the beginning and end of the oil lubricity test
W	mechanical work
$WS_{1,4}$	HFFR normalized wear scar diameter (lubricity)
WSD	uncorrected average wear scar diameter
x	HFFR wear scar diameter perpendicular to the direction of oscillation
y	HFFR wear scar diameter in a direction parallel to the direction of oscillation.
ε	coefficient of change in the density of the substance when heated by 1 °C
λ	thermal conductivity coefficient
η	dynamic viscosity of a fluid
μ	friction coefficient

ν	kinematic viscosity of a lubricant
ρ	lubricant density
τ	working time

Appendix A. Mathematical Derivation of Relation between Unit Heat Flux and Sliding Velocity

If two bodies, X and Y, are in contact and body X moves relative to body Y, mechanical work is required to perform this motion (transferring energy to body X from an external source). This relationship is described by the following equation:

$$W = Fs, \quad (A1)$$

where F is the magnitude of the sliding force and s is the distance over which body X slides on body Y.

Sliding motion requires the overcoming of frictional resistance T_F , so the force F is equal in magnitude to the frictional force between bodies X and Y. It has the same direction as the force F but is opposite in sense (for the purpose of these calculations, we are interested in the absolute value since work is a scalar quantity). Therefore, Equation (A1) can be written as:

$$W = T_R s. \quad (A2)$$

The sliding friction force can be described as:

$$T_R = P\mu, \quad (A3)$$

where P is the normal force exerted by body X on body Y and μ is the coefficient of sliding friction between body X and Y under the given operating conditions.

Next, by substituting Equation (A3) into Equation (A2), we obtain:

$$W = P\mu s. \quad (A4)$$

If all the mechanical energy is converted into thermal energy Q , then $Q = W$. Therefore, Equation (A4) can be rewritten as:

$$Q = P\mu s. \quad (A5)$$

If we divide both sides of Equation (A5) by time τ , we obtain:

$$\frac{Q}{\tau} = P\mu \frac{s}{\tau}. \quad (A6)$$

The heat flux is defined as $\dot{Q} = \frac{Q}{\tau}$ and the sliding velocity can be described as $C_m = \frac{s}{\tau}$. Therefore, Equation (A6) can be presented in the following form:

$$\dot{Q} = C_m P\mu. \quad (A7)$$

By dividing both sides of Equation (A7) by the heat transfer area A (in units m^2), which corresponds to the contact surface area between body X and body Y, the heat flux \dot{Q} (W) is converted to the unit heat flux $\dot{q} = \frac{\dot{Q}}{A}$ with dimensions $\text{J}/(\text{s} \cdot \text{m}^2) = \text{W}/\text{m}^2$, and the force P (N) is converted to the unit pressure $p = \frac{P}{A}$ with dimensions $\text{Pa} = \text{N}/\text{m}^2$. Furthermore, by substituting using the relationship $S_{gr} = C_m p$, we obtain the complete formula presented in this article as Equation (4), i.e.,:

$$\dot{q} = C_m p \mu = S_{gr} \mu. \quad (A8)$$

Appendix B. Measurement Data Obtained in the Experiment

Table A1. SAE 30 grade lubricating oil mixtures.

Diesel Oil Content (% m/m)	Lubricating Oil SAE 30 with DO Mixes									
	0	1	2	5	10	20	30	40	50	75
Kinematic viscosity ν @100 °C (mm ² /s)	11.72	11.05	10.96	10.32	8.40	6.40	4.82	3.70	3.01	1.86
Dynamic viscosity η @100 °C (mPa·s)	9.91	9.33	9.25	8.69	7.04	5.32	3.97	3.03	2.44	1.48
Viscosity index VI (—)	99.3	97.3	97.6	107.0	111.5	129.2	122.2	127.1	132.6	149.9
Density ρ @100 °C (kg/m ³)	845.42	844.16	843.91	841.72	838.07	830.97	824.49	817.34	809.72	793.92
Coefficient of temperature density change ε (kg/(m ³ ·K))	0.622	0.624	0.625	0.627	0.630	0.639	0.645	0.662	0.666	0.681
HFFR x wear scar diameter (μ m)	156	231	213	227	243	69	150	144	154	309
HFFR y wear scar diameter (μ m)	194	149	135	157	126	98	151	141	122	302
HFFR average wear scar diameter WSD (μ m)	175.0	190.0	174.0	192.0	184.5	83.5	150.5	142.5	138.0	305.5
HFFR normalized wear scar diameter (lubricity) $WS_{1.4}$ (μ m)	182	196	173	205	197	100	188	178	152	339
HFFR mean friction coefficient μ (—)	0.139	0.139	0.139	0.137	0.138	0.146	0.146	0.149	0.150	0.175
HFFR oil film resistance $FILM$ (%)	100	100	100	100	100	99	96	97	97	58
Flash point temperature t_{FP} (°C)	180.0	166.0	160.0	134.0	110.0	96.0	79.5	72.5	78.0	62.5
Cetane index CII acc. ASTM D4737	N/A	N/A	N/A	N/A	N/A	N/A	47.8	50.4	52.4	51.5

Table A2. SAE 40 grade lubricating oil mixtures.

Diesel Oil Content (% m/m)	Lubricating Oil SAE 40 with DO Mixes									
	0	1	2	5	10	20	30	40	50	75
Kinematic viscosity ν @100 °C (mm ² /s)	15.21	15.05	14.51	12.90	10.24	7.91	5.61	4.27	3.45	1.97
Dynamic viscosity η @100 °C (mPa·s)	12.87	12.72	12.25	10.87	8.58	6.58	4.63	3.49	2.79	1.57
Viscosity index VI (—)	95.3	94.9	95.2	96.5	112.7	125.8	133.3	135.2	142.3	161.1
Density ρ @100 °C (kg/m ³)	846.04	845.45	844.58	842.43	838.35	832.13	824.41	817.43	810.31	793.48
Coefficient of temperature density change ε (kg/(m ³ ·K))	0.616	0.613	0.615	0.620	0.621	0.628	0.643	0.651	0.660	0.684
HFFR x wear scar diameter (μ m)	219	199	213	199	127	89	165	217	227	179
HFFR y wear scar diameter (μ m)	132	105	131	152	138	112	126	176	123	177
HFFR average wear scar diameter WSD (μ m)	175.5	152.0	172.0	175.5	132.5	100.5	145.5	196.5	175.0	178.0
HFFR normalized wear scar diameter (lubricity) $WS_{1.4}$ (μ m)	176	151	173	176	141	107	192	245	191	227
HFFR mean friction coefficient μ (—)	0.132	0.134	0.135	0.133	0.133	0.136	0.137	0.146	0.152	0.152
HFFR oil film resistance $FILM$ (%)	100	100	100	100	100	96	91	85	78	83
Flash point temperature t_{FP} (°C)	178	160	150	132	100	93	77.5	75.5	74	62.5
Cetane index CII acc. ASTM D4737	N/A	N/A	N/A	N/A	N/A	N/A	N/A	49.2	52.1	48.9

Appendix C. HFFR Apparatus Data

Table A3. Technical data of the HFFR V1.0.3 and HFR2 set for lubricity measurement (prepared based on refs [68,69]).

Parameter	Value
Mechanical part	
Oscillation frequency	10–220 Hz
Oscillation pitch	20–2000 μ m
Load (replaceable weights)	0–1.0 kg
The maximum friction force depends on the amplitude	10.0 N
Standard samples	
Ball diameter (top sample)	6.0 mm
Plate diameter (bottom sample)	10.0 mm
Plate thickness (bottom sample)	3.0 mm

Table A3. Cont.

Parameter	Value
Temperature control and heater	
Adjustment range	0–200 °C
Main temperature sensor	Pt 100 in a stainless steel sheath
Alarm temperature sensor	Pt 100 in a stainless steel sheath
Heating elements	2 pcs, 24 V, 15 W
Maximum temperature without additional heating	~120 °C above ambient temperature
Power supply and measurement system	
The initial voltage of the polarization in the measurement system of the electrical contact resistance of the samples	15 mV
Force measurement accuracy	<0.35% of the measuring range
Main power	240 V, 50 Hz, 400 W
Overcurrent protection	3.15 A, fuse, 20 mm
HFR2 microscope	
Microscope magnification with standard lenses	100×
Microscope measurement resolution	1 µm
Supply voltage	240 V, 50 Hz

References

- Wiaterek, D.; Chybowski, L. Assessing the topicality of the problem related to the explosion of crankcases in marine main propulsion engines (1972–2018). *Sci. J. Marit. Univ. Szczec.* **2022**, *71*, 33–40.
- Borkowski, T.; Kowalak, P.; Myśków, J. Vessel main propulsion engine performance evaluation. *J. KONES* **2012**, *19*, 53–60. [CrossRef]
- Kowalak, P.; Myśków, J.; Tuński, T.; Bykowski, D.; Borkowski, T. A method for assessing of ship fuel system failures resulting from fuel changeover imposed by environmental requirements. *Eksploat. Niezawodn.—Maint. Reliab.* **2021**, *23*, 619–626. [CrossRef]
- Szczepanek, M. Biofuels as an alternative fuel for West Pomeranian fishing fleet. *J. Phys. Conf. Ser.* **2019**, *1172*, 012074. [CrossRef]
- Zhang, Y.; Ma, Z.; Feng, Y.; Diao, Z.; Liu, Z. The Effects of Ultra-Low Viscosity Engine Oil on Mechanical Efficiency and Fuel Economy. *Energies* **2021**, *14*, 2320. [CrossRef]
- Ferguson, G.W. *Diesel Engine Crankcase Explosion Investigation*; Technical Paper 510104; SAE International: Warrendale, PA, USA, 1951; pp. 1–28. [CrossRef]
- CIMAC. *Guideline on the Relevance of Lubrication Flash Point in Connection with Crankcase Explosions*; CIMAC Working Group 8 “Marine Lubricants”: Frankfurt, Germany, 2013.
- Graddage, M. Crankcase Explosions—Detection or Prevention? In *Crankcase Explosions*; IMAREST: London, UK, 2002; pp. 126–147.
- Metalock Engineering UK. Crankcase Explosion. Following Catastrophic Engine Failure When a Con-Rod Breaks through the Crankcase Door, Water Jacket and Liner Area, Does This Mean a New Engineblock? Available online: <https://www.metalockengineering.com/en/metalock-engineering-uk-limited/news/crankcase-explosion/> (accessed on 20 June 2022).
- Cicek, K.; Celik, M. Application of failure modes and effects analysis to main engine crankcase explosion failure on-board ship. *Saf. Sci.* **2013**, *51*, 6–10. [CrossRef]
- Technomics International. Case Study—Fuel Dilution of Engine Oil in Locomotives. Available online: <https://www.technomics.net/case-studies/fuel-dilution-engine-oil/> (accessed on 8 June 2022).
- Krupowies, J. *Badania Zmian Parametrów Fizykochemicznych Silnikowych Olejów Smarowych Eksploatowanych na Statkach Polskiej Żeglugi Morskiej*; Studia Nr.; Wyższa Szkoła Morska w Szczecinie: Szczecin, Poland, 1996.
- Castrol. Oil Contamination Identification. A List of the Top Offenders. Available online: https://www.castrol.com/content/dam/castrol/country-sites/en_us/united-states/home/hd-focus-newsletter/labcheck-oil-contamination-infographic.pdf (accessed on 7 June 2023).
- Gearhead Oil Analysis. Engine Oil Analysis. Available online: <https://shop.gearheadlab.com/pages/engine-oil-analysis> (accessed on 7 June 2023).
- Chybowski, L. The Initial Boiling Point of Lubricating Oil as an Indicator for the Assessment of the Possible Contamination of Lubricating Oil with Diesel Oil. *Energies* **2022**, *15*, 7927. [CrossRef]
- Chybowski, L. Study of the Relationship between the Level of Lubricating Oil Contamination with Distillation Fuel and the Risk of Explosion in the Crankcase of a Marine Trunk Type Engine. *Energies* **2023**, *16*, 683. [CrossRef]
- Sejkorová, M.; Hurtová, I.; Jilek, P.; Novák, M.; Voltr, O. Study of the Effect of Physicochemical Degradation and Contamination of Motor Oils on Their Lubricity. *Coatings* **2021**, *11*, 60. [CrossRef]

18. Winterbone, D.E.; Turan, A. *Advanced Thermodynamics for Engineers*; Elsevier: Amsterdam, The Netherlands, 2015; ISBN 9780444633736.
19. Włodarski, J.; Podsiadło, A.; Kluj, S. *Uszkodzenia Systemu Tłok-Cylinder (TC) Okrętowych Silników Spalinowych*; Wydawnictwo Akademii Morskiej w Gdyni: Gdynia, Poland, 2011.
20. Gawdzińska, K.; Chybowski, L.; Bejger, A.; Krile, S. Determination of technological parameters of saturated composites based on sic by means of a model liquid. *Metallurgija* **2016**, *55*, 659–662.
21. Ratajczak, M.; Ptak, M.; Chybowski, L.; Gawdzińska, K.; Będziński, R. Material and Structural Modeling Aspects of Brain Tissue Deformation under Dynamic Loads. *Materials* **2019**, *12*, 271. [[CrossRef](#)] [[PubMed](#)]
22. Kozaczewski, W. *Konstrukcja Grupy Tłokowo-Cylindrowej Silników Spalinowych*; WKiŁ: Warszawa, Poland, 2004.
23. Chybowski, L.; Szczepanek, M.; Gawdzińska, K.; Klyus, O. Particles Morphology of Mechanically Generated Oil Mist Mixtures of SAE 40 Grade Lubricating Oil with Diesel Oil in the Context of Explosion Risk in the Crankcase of a Marine Engine. *Energies* **2023**, *16*, 3915. [[CrossRef](#)]
24. Chybowski, L. *Lube Oil—Diesel Oil Mixes—Dataset*; Maritime University of Szczecin: Szczecin, Poland, 2022; Version 3.
25. PKN Orlen, S.A. *Olej Napędowy. Ecodiesel Ultra B,D,F, Olej Napędowy Arktyczny Klasy 2, Efecta Diesel B,D,F, Verva ON B,D,F*; PKN Orlen S.A.: Płock, Poland, 2021.
26. Minister Gospodarki, R.P. *Rozporządzenie Ministra Gospodarki z Dnia 9 Października 2015 r. w Sprawie Wymagań Jakościowych Dla paliw Ciekłych*; Ministerstwo Gospodarki RP: Warszawa, Poland, 2015.
27. PKN Orlen, S.A. *ZN-ORLEN-5—Przetwory naftowe. Olej Napędowy Efecta Diesel*; PKN Orlen S.A.: Płock, Poland, 2019.
28. Society of Automotive Engineers. *SAE J300-2021. Engine Oil Viscosity Classification*; SAE International: Warrendale, PA, USA, 2021.
29. *DIN 51794:2003-05*; Testing of Mineral Oil Hydrocarbons—Determination of Ignition Temperature. German Institute for Standardisation (Deutsches Institut für Normung): Berlin, Germany, 2003.
30. *PN-EN ISO 3104:2021-03*; Petroleum Products—Transparent and Opaque Liquids—Determination of Kinematic Viscosity and Calculation of Dynamic Viscosity. PKN: Warszawa, Poland, 2021.
31. Oleje-Smary. AGIP Cladium 120 SAE 30 CD. Available online: <https://oleje-smary.pl/pl/p/AGIP-Cladium-120-SAE-30-CD-20-litrow/186> (accessed on 12 July 2022).
32. Oleje-Smary. AGIP Cladium 120 SAE 40 CD. Available online: <https://oleje-smary.pl/pl/p/AGIP-Cladium-120-SAE-40-CD-20-litrow/188> (accessed on 12 July 2022).
33. ITALCO (Far East) Pte Ltd. *Product Data Sheet—Eni Cladium 120 (Series)*; ITALCO: Singapore, 2017.
34. *ISO 2719:2016*; Determination of Flash Point—Pensky-Martens Closed Cup Method. 4th ed. ISO: Geneva, Switzerland, 2016.
35. *ASTM D4737-21*; Standard Test Method for Calculated Cetane Index by Four Variable Equation. ASTM: West Conshohocken, PA, USA, 2021.
36. *PN-EN ISO 12185:2002*; Ropa naftowa i przetwory naftowe—Oznaczanie gęstości—Metoda oscylacyjna z U-rurką. PKN: Warszawa, Poland, 2002.
37. *ASTM D 2270-10(2016)*; Standard Practice for Calculating Viscosity Index from Kinematic Viscosity at 40 °C and 100 °C. ASTM: West Conshohocken, PA, USA, 2016.
38. *EN ISO 12156-1:2018*; Diesel Fuel—Assesment of Lubricity Using the High-Frequency Reciporating Rig (HFFR)—Part 1: Test Method. ISO: Geneva, Switzerland, 2018.
39. *PN-EN IEC 60079-10-1:2021-09*; Explosive Atmospheres—Part 10-1: Classification of Areas—Explosive Gas Atmospheres. PKN: Warszawa, Poland, 2021.
40. Krupowies, J. *Badania Zmian Właściwości Oleju Obiegowego Okrętowych Silników Pomocniczych*; Wyższa Szkoła Morska w Szczecinie: Szczecin, Poland, 2002.
41. Anish. Important Lube Oil Properties to Be Considered While Choosing Marine Lube Oil for Your Ship. Available online: <https://www.marineinsight.com/guidelines/important-lube-oil-properties-to-be-considered-while-choosing-marine-lube-oil-for-your-ship/> (accessed on 20 June 2023).
42. Krupowies, J. *Badania i Ocena Zmian Właściwości Użytkowych Olejów Urządzeń Okrętowych*; Maritime University of Szczecin: Szczecin, Poland, 2009.
43. Ramadan, O.; Menard, L.; Gardiner, D.; Wilcox, A.; Webster, G. *Performance Evaluation of the Ignition Quality Testers Equipped with TALM Precision Package (TALM-IQT™) Participating in the ASTM NEG Cetane Number Fuel Exchange Program*; Technical Paper 2017-01-0720; SAE International: Warrendale, PA, USA, 2017. [[CrossRef](#)]
44. PAC. *Aparat Do Oznaczania Pochodnej Liczby Cetanowej*; Inkom Instruments Co.: Warszawa, Poland, 2008.
45. PAC L.P. *Herzog Cetane ID 510*; PAC L.P.: Houston, TX, USA, 2019.
46. Yanowitz, J.; McCormick, R.L. Review: Fuel Volatility Standards and Spark-Ignition Vehicle Driveability. *SAE Int. J. Fuels Lubr.* **2016**, *9*, 408–429. [[CrossRef](#)]
47. Chybowski, L.; Grzadziel, Z.; Gawdzińska, K. Simulation and experimental studies of a multi-tubular floating sea wave damper. *Energies* **2018**, *11*, 1012. [[CrossRef](#)]
48. Kaminski, P. Experimental Investigation into the Effects of Fuel Dilution on the Change in Chemical Properties of Lubricating Oil Used in Fuel Injection Pump of Pielstick PA4 V185 Marine Diesel Engine. *Lubricants* **2022**, *10*, 162. [[CrossRef](#)]
49. Stone, A.S. New low viscosity grade engine oil specification rises from the ashes of category development delays. *Fuels Lubes Int.* **2017**, *23*, 18–21.

50. Martyr, A.J.; Plint, M.A. *Engine Testing*; Elsevier: Amsterdam, The Netherlands, 2012; ISBN 9780080969497.
51. Oilmanager. Oil Viscosity and Its Importance. Available online: <https://www.techenomics.net/2014/02/oil-viscosity-and-its-importance/> (accessed on 20 June 2023).
52. Chybowski, L.; Myśków, J.; Kowalak, P. Analysis of fuel properties in the context of the causes of three marine auxiliary engines failure—A case study. *Eng. Fail. Anal.* **2023**, *150*, 107362. [CrossRef]
53. Anton Paar. ASTM D 2270—Viscosity Index (VI) from 40 °C and 100 °C. Available online: <https://wiki.anton-paar.com/pl-pl/wskaznik-lepkosci-vi-od-40c-i-100c-astm-d2270/> (accessed on 7 September 2022).
54. Piotrowski, I.; Witkowski, K. *Określenie Silniki Spalinowe*, 3rd ed.; Trademar: Gdynia, Poland, 2013; ISBN 978-83-62227-48-8.
55. Kolm, R.; Gebeshuber, I.C.; Kenesey, E.; Ecker, A.; Pauschitz, A.; Werner, W.S.M.; Störi, H. Tribochemistry of mono molecular additive films on metal surfaces, investigated by XPS and HFRR. *Tribol. Interface Eng. Ser.* **2005**, *48*, 269–282. [CrossRef]
56. Malinowska, M.; Zera, D. Analiza zmian smarności oleju silnikowego stosowanego w silniku Cegielski-Sulzer 3AL25/30. *Zesz. Nauk. Akad. Mor. W Gdyni* **2016**, *96*, 93–104.
57. Mikołajczyk, J. *Tribotestery. Budowa i Przeznaczenie*; Wydawnictwo Państwowej Wyższej Szkoły Zawodowej im. Stanisława Staszica w Pile: Piła, Poland, 2019.
58. Total Polska Sp., z.o.o. *Przemysłowe Środki Smarne—Poradnik*; Total Polska Sp. z.o.o.: Warszawa, Poland, 2003.
59. Bhatia, S.C. Biodiesel. In *Advanced Renewable Energy Systems*; Elsevier: Amsterdam, The Netherlands, 2014; pp. 573–626.
60. InSight. Research Confirms HFRR Is the Best Test to Accurately Measure Diesel Fuel Lubricity. Available online: <http://www.infineuminsight.com/insight/dec-2013/testing-the-test> (accessed on 5 May 2018).
61. ASTM D 6079; Standard Test Method for Evaluating Lubricity of Diesel Fuels by the High-Frequency Reciprocating Rig (HFRR). ASTM: West Conshohocken, PA, USA, 2023.
62. Cursaru, D.; Sorin, V.; Mihai, S.; Ghiță, D.; Stoica, S.-D.; Dinescu, G. Friction and wear properties of carbon nanowalls coatings. *Dig. J. Nanomater. Biostructures* **2014**, *9*, 1105–1114.
63. PN-EN ISO 12156-1:2008; Oleje Napędowe—Ocena Smarności z Zastosowaniem Aparatu o Ruchu Posuwisto-Zwrotnym Wysokiej Częstotliwości (HFRR)—Część 1: Metoda Badania. PKN: Warszawa, Poland, 2006.
64. Nozdrzykowski, K.; Adamczak, S.; Grządziel, Z.; Dunaj, P. The Effect of Deflections and Elastic Deformations on Geometrical Deviation and Shape Profile Measurements of Large Crankshafts with Uncontrolled Supports. *Sensors* **2020**, *20*, 5714. [CrossRef] [PubMed]
65. Włodarski, J. *Tłokowe Silniki Spalinowe—Procesy Trybologiczne*; WKiŁ: Warszawa, Poland, 1982.
66. Ashgriz, N. *Handbook of Atomization and Sprays*; Ashgriz, N., Ed.; Springer: Boston, MA, USA, 2011; ISBN 978-1-4419-7263-7.
67. ASTM D 7668; Standard Test Method for Determination of Derived Cetane Number (DCN) of Diesel Fuel Oils Ignition Delay and Combustion Delay Using a Constant Volume Combustion Chamber Method. ASTM: West Conshohocken, PA, USA, 2010.
68. PCS Instruments. *Aparat Do Badania Paliw i Środków Smarnych. Instrukcja Obsługi Systemu HFRR V1.0.3*; Inkom Instruments Co.: Warszawa, Poland, n.d.
69. PCS Instruments. *Instrukcja Obsługi, Mikroskop Do Pomiaru Skazy Zużycia Na Aparacie HFR2*; Inkom Instruments Co.: Warszawa, Poland, 1999.

Disclaimer/Publisher’s Note: The statements, opinions and data contained in all publications are solely those of the individual author(s) and contributor(s) and not of MDPI and/or the editor(s). MDPI and/or the editor(s) disclaim responsibility for any injury to people or property resulting from any ideas, methods, instructions or products referred to in the content.